Observation of "Intramolecular" Ion–Molecule Reactions within Ionized Clusters: Hetero Systems Involving Methyl Halides and Oxygen-Containing Compounds

James F. Garvey and Richard B. Bernstein*

Contribution from the Department of Chemistry and Biochemistry, University of California, Los Angeles, California 90024. *Received August 5, 1986*

Abstract: "Intramolecular" ion–molecule reactions are observed following electron impact ionization of heterocluster beams of methyl halides with oxy compounds. The resulting fragmentation patterns reveal the mechanisms of these reactions: extensive intramolecular rearrangements occur *within* the excited, solvated cation. The major reactive processes can be rationalized in terms of intramolecular analogues of known gas-phase, bimolecular ion–molecule reactions, such as the protonation reaction $M_nA_m^+ \rightarrow M_{n-1}A_mH^+ + CH_2X$ (where M = methyl halide, X = Cl or I, and A = oxy compound). Here A includes $(CH_3)_2CO$, CH_3OH, H_2O (and their perdeuteriated analogues), and $(CH_3)_2O$. Several novel reactive pathways have been inferred from the cluster ion mass spectra. From observation of the dependence of reaction yields and relative rate constants upon cluster size it is evident that even a few "solvent" molecules on the cation suffice to alter the course of the reaction. For neat clusters the protonation rates decrease as cluster size increases. This can be explained by the increased stability of the ion (with increasing cluster size n), hence an increasing barrier to reaction as a function of n. In the case of the heterocluster ions this trend is reversed: the rates of analogous ion–molecule reactions are faster than those for the neat cluster ions, and these rates increase with n. These results can also be explained by energetic considerations.

1. Introduction

A subject of intense interest in recent years has been the study of the physics of weakly bound van der Waals molecules (clusters) produced in expanding jets. These species have been probed in a variety of ways to gain an understanding of their formation and to determine their various properties. However, chemical reactions involving clusters have only recently attracted attention. This aspect of cluster science is especially intriguing to the chemist since the study of reactions within clusters may serve to join the disparate fields of bimolecular gas-phase reaction dynamics and solution chemistry. Most of this recent work consists of utilizing the neutral cluster as one of the reagents for a bimolecular reaction.[1-8] Apart from the observation of protonated clusters, e.g., $(H_2O)_nH^+$,[9] $(NH_3)_nH^+$,[10,11] $(CH_3CHOCH_3)_nH^+$,[12] $(CH_3OH)_nH^+$,[13] $(CH_3OCH_3)_nH^+$,[13] and a few heterocluster ions such as $[(ROH)_n(H_2O)_m]H^+$[14,15] and $[(CH_3CH)_n(H_2O)_m]H^+$,[16] there are few reported cases of chemical reactions taking place within the cluster ion itself.[12,16-20] Nevertheless, it is known that electron impact (EI) ionization of clusters leads to ions that closely resemble many of the intermediates found in bimolecular ion–molecule reactions.[21,22] Yet up to now ionization of clusters has been used primarily in connection with mass spectrometric experiments designed to ascertain the size distribution within cluster beams.

When ionized, large polyatomics[23,24] (such as halohydrocarbons[25-27]) are internally excited, and the randomized excess

Chart I

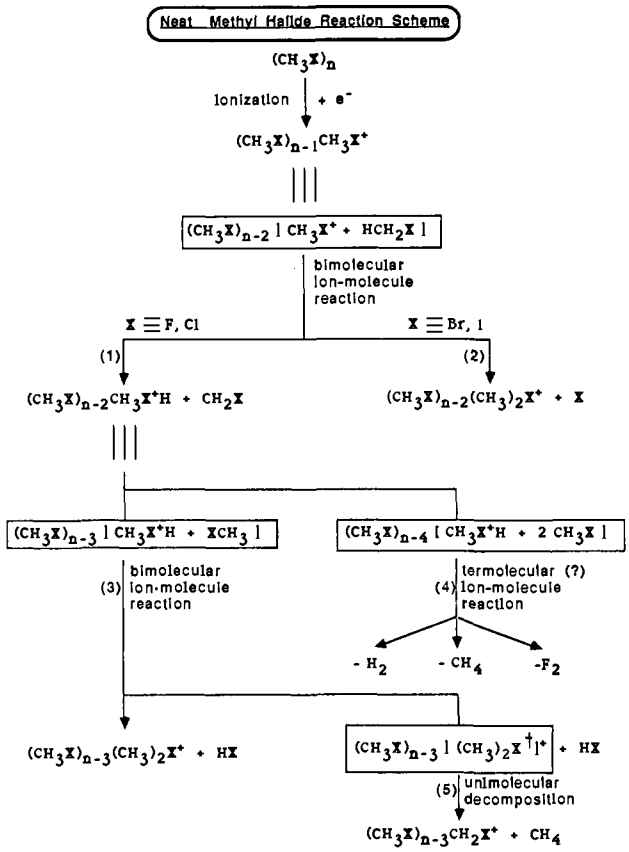

When ionized, large polyatomics[23,24] (such as halohydrocarbons[25-27]) are internally excited, and the randomized excess

(1) Whitehead, J. C.; Grice, R. *Faraday Discuss. Chem. Soc.* **1973**, *55*, 320.
(2) King, D. L.; Dixon, D. A.; Herschbach, D. R. *J. Am. Chem. Soc.* **1974**, *96*, 3328.
(3) González Ureña, A.; Bernstein, R. B.; Phillips, G. R. *J. Chem. Phys.* **1975**, *62*, 1818.
(4) Behrens, R. B., Jr.; Freedman, A.; Herm, R. R.; Parr, T. P. *J. Chem. Phys.* **1975**, *63*, 4622.
(5) Wren, D. J.; Menzinger, M. *Chem. Phys.* **1982**, *66*, 85.
(6) Nieman, J.; Na'aman, R. *Chem. Phys.* **1984**, *90*, 407.
(7) Morse, M. D.; Smalley, R. E. *Ber. Bunsenges. Phys. Chem.* **1984**, *88*, 208.
(8) Whetten, R. L.; Cox, D. M.; Trevor, D. J.; Kaldor, A. *Surf. Sci.* **1985**, *156*, 8.
(9) Hermann, V.; Kay, B. D.; Castleman, A. W., Jr. *Chem. Phys.* **1982**, *72*, 185.
(10) Stephan, K.; Futrell, J. H.; Peterson, K. I.; Castleman, A. W., Jr.; Wagner, H. E.; Djuric, N.; Mark, T. D. *Int. J. Mass Spectrom. Ion Phys.* **1962**, *44*, 167.
(11) Echt, O.; Morgan, S.; Dao, P. D.; Stanley, R. J.; Castleman, A. W. Jr. *Ber. Bunsenges. Phys. Chem.* **1984**, *88*, 217.
(12) Stace, A. J.; Shukla, A. K. *J. Phys. Chem.* **1982**, *86*, 865.
(13) Grimsrud, E. P.; Kebarle, P. *J. Am. Chem. Soc.* **1973**, *95*, 7939.
(14) Stace, A. J.; Shukla, A. K. *J. Am. Chem. Soc.* **1982**, *82*, 5314.
(15) Stace, A. J.; Moore, C. *J. Am. Chem. Soc.* **1983**, *83*, 1814.
(16) Kenny, J. E.; Brumbaugh, D. V.; Levy, D. H. *J. Chem. Phys.* **1979**, *71*, 4757.
(17) (a) Klots, C. E.; Compton, R. N. *J. Chem. Phys.* **1978**, *69*, 1644. (b) Klots, C. E. *Radiat. Phys. Chem.* **1982**, *20*, 51. (c) Klots, C. E. *Kinetics of Ion-Molecule Reactions*; Ausloos, P., Ed.; Plenum: New York, 1979; p 69.
(18) Ono, Y.; Ng, C. Y. *J. Am. Chem. Soc.* **1982**, *104*, 4752.
(19) Nishi, N.; Yamamoto, K.; Shinohara, H.; Nagashima, U.; Okuyama, T. *Chem. Phys. Lett.* **1985**, *122*, 599.
(20) Stace, A. J. *J. Am. Chem. Soc.* **1985**, *107*, 755.
(21) Milne, T. A.; Beachey, J. E.; Greene, F. T. *J. Chem. Phys.* **1972**, *56*, 3007.
(22) Ceyer, S. T.; Tiedemann, P. W.; Ng, C. Y.; Mahan, B. H.; Lee, Y. T. *J. Chem. Phys.* **1979**, *70*, 2138.
(23) Mansell, P. I.; Danby, C. J.; Powis, I. *J. Chem. Soc., Faraday Trans. 1* **1981**, *77*, 1449.

0002-7863/87/1509-1921$01.50/0

energy can initiate bond cleavage, with this ion fragment distribution being well accounted for by the quasi-equilibrium theory. One might have expected an ionized cluster to exhibit unimolecular decay in a similar fashion. In contrast, extensive bond reformation takes place within these ionized clusters (as reported for methyl halide systems[28,29]). This suggests that bimolecular (and possibly termolecular) chemical reactions are occurring *within* a given cluster ion (here a solvated cation). The major reactive pathways observed[28,29] could be accounted for by known bimolecular ion–molecule reactions, observed previously in conventional ICR experiments[30–34] and via high-pressure mass spectrometry.[13] Our results[29] for neat methyl halide clusters are summarized in the following reactive scheme (Chart I).

For the case of the CH_3F clusters, the experiments[29] strongly suggested a reaction mechanism in which the energized cluster ion ejects CH_2F (step 1) with the formation of a protonated cluster (with one less monomer unit). The bimolecular analogue is $CH_3F^+ + CH_3F \rightarrow CH_3FH^+ + CHF_2$, a well-known exothermic ion–molecule reaction (which may have also been recently observed in photoionization experiments of CH_3F clusters[35]).

In the case of the CH_3Cl clusters, this hydrogen-transfer reaction occurs with a lower rate, such that the "parent" ion (reactant) and the protonated cluster ion (product) are both present in comparable abundances. However, the bimolecular gas-phase reactions for both the CH_3F and CH_3Cl systems exhibit the same rates.[32]

This certainly is not the case inside a cluster and suggests a barrier to reaction in the cluster, absent in the bimolecular case. This observation serves as a cautionary example regarding the difficulty of transferring results from the gas phase to the cluster, much less the condensed phase. Finally, for the CH_3Br and CH_3I clusters (for which the analogous bimolecular reactions are endothermic), the protonation reaction is not observed. What is found instead is the ejection of a halogen atom via a nucleophilic displacement reaction (step 2) to produce a halonium cluster ion. (The bimolecular analogue reaction is also well known.[32]) Thus the cluster ion chemistry of the methyl halides is entirely systematic.

In the case of the CH_3Cl clusters, since both reactant and protonated product ions can be observed, it has been possible to estimate the dependence of the protonation reaction (step 1) rate constant upon cluster size.[29] From dimer to trimer the relative rate of reaction drops by 25%, from dimer to tetramer it drops by 40%. Thus the stepwise solvation of one or two molecules effectively damps out this otherwise facile hydrogen-transfer reaction. This dramatic solvent effect implies that very few molecules acting as "spectators" (energy sinks) suffice to exert striking dynamical effects.

We also observe that, for those systems producing a protonated ion (CH_3XH^+) solvated by the other CH_3X molecules in the cluster, further bimolecular (step 3) and possibly termolecular (step 4) reactions can occur, with the ejection of neutral, closed-shell molecules. Some of the molecular cluster ions generated in this fashion may be vibrationally excited (due to the exothermicity of the previous reaction) and can decay unimolecularly by the further ejection of closed-shell neutrals (step 5). However, for the CH_3F and CH_3Cl systems, we also observe neutral molecule formation that has absolutely no counterpart in the gas-phase bimolecular reactions, occurring only in the unique "solvated" environment of the cluster (step 4).

These experiments have revealed a new class of unimolecular reactions that can best be described as bimolecular (and termolecular?) ion–molecule reactions occurring within the solvated environs in a cluster. We can study in detail the role played by ion solvation in the reaction dynamics within the cluster ions.

We have now extended our studies to heterocluster systems (e.g., M_nA_m where M = CH_3X; A = $(CH_3)_2O$, $(CH_3)_2CO$, CH_3OH, H_2O; X = Cl, I) to look for new intramolecular ion–molecule reactions (occurring within the ionized clusters) and elucidate reactive pathways not ordinarily found in bimolecular ion–molecule collisions. (We have also employed the perdeuteriated analogues of several of the oxy molecules in order to trace the various ion–molecule reaction pathways.) These heterosystems are of interest since (in contrast to the homocluster case) the ion generated finds two kinds of molecules from which to abstract a hydrogen. Observation of the branching ratios yields rate constant ratios which are indicative of differences in hydrogen affinity for ions within a cluster.

The main questions we now wish to address are as follows: (a) To what degree can current knowledge about gas-phase ion–molecule reactions be applied to explain such reactions occurring *within* the cluster ions, and under what circumstances is it inadequate? (b) How are these elementary reactions influenced by stepwise solvation (i.e., increasing cluster size)? (c) How do the rates of reactions occurring "inside" the clusters compare with those for the bimolecular analogues? (d) What are the differences between the reactions within heterocluster ions and homocluster (neat) ions?

Thus the study of reactive processes in cluster ions may be used eventually as a bridge between the gas-phase (bimolecular) and the solvated world of ionic reactions in solution.[36] Observations of novel reactive pathways and unexpected dynamics within cluster ions demonstrate the profound effect that only a few solvent molecules have on the course of a reaction. It will be seen from the experimental results below how very quickly, with increasing solvation, one leaves the bimolecular world.

2. Experimental Section

A complete description of the apparatus used in this investigation has been published.[29] In the present study neutral (M_nA_m) cluster beams are formed by adiabatic expansion of a suitable vapor mixture[37] through a 50-μm diameter nozzle at 29 °C into a chamber at a pressure $<5 \times 10^{-4}$ torr. After collimation by a 0.5-mm diameter skimmer, the molecular beam passes through a 0.3-m differentially pumped "transition" chamber ($P < 1 \times 10^{-6}$ torr) and then travels through an additional 1-m chamber ($P < 1 \times 10^{-7}$ torr) before being ionized by electron impact (EI) and mass analyzed on a Dycor M200M quadrupole mass spectrometer with a channel-plate ion–electron multiplier. This instrument is provided with a computerized data acquisition system, which allows subtraction of residual background mass spectra. All results presented here were obtained at unit mass resolution up to m/z 200. The operating system has already been described.[29]

3. Results and Discussion

For all the heterocluster beams the mass spectra are extensive and complex. Nevertheless, mass assignments and empirical formulas have been deduced for the ions corresponding to all the major peaks, with almost all peaks assigned. In the figures that follow, the mass spectra shown for each system are typical of many, recorded under varying conditions of sensitivity and resolution. All peaks whose assignments are given have been observed consistently in several confirmatory mass spectra.

In each case all the identified ion peaks have been accounted

(24) Baer, T.; DePristo, A. E.; Hermans, J. J. *J. Chem. Phys.* **1981**, *76*, 1449.
(25) Simm, I. G.; Danby, C. J. *J. Chem. Soc., Faraday Trans. 1* **1976**, *77*, 861.
(26) Powis, I.; Danby, C. J. *Chem. Phys. Lett.* **1979**, *65*, 390.
(27) Powis, I. *Mol. Phys.* **1980**, *34*, 311.
(28) Garvey, J. F.; Bernstein, R. B. *Chem. Phys. Lett.* **1986**, *126*, 394.
(29) Garvey, J. F.; Bernstein, R. B. *J. Phys. Chem.* **1986**, *90*, 3577.
(30) McAskill, N. A.; *Aust. J. Chem.* **1970**, *23*, 2301.
(31) Herod, A. A.; Harrison, A. G.; McAskill, N. A. *Can. J. Chem.* **1971**, *49*, 2217.
(32) Beauchamp, J. L.; Holtz, D.; Woodgate, S. D.; Patt, S. L. *J. Am. Chem. Soc.* **1972**, *94*, 2798.
(33) McMahon, T. B.; Blint, R. J.; Ridge, D. P.; Beauchamp, J. L. *J. Am. Chem. Soc.* **1972**, *94*, 8934.
(34) Blint, R. J.; McMahon, T. B.; Beauchamp, J. L. *J. Am. Chem. Soc.* **1974**, *96*, 1269.
(35) Ruhl, E.; Bisling, P.; Brutschy, B.; Baumgärtel, H. *Bessy. Annual Report 124*, 1985.
(36) Bohme, D. K. *NATO ASI Ser., Ser. C* **1984**, *118*, 111.
(37) Here A = CH_3OH, CD_3OD, CH_3OCH_3, CH_3COCH_3, CD_3COCD_3, H_2O, D_2O, and M = CH_3X where X = Cl or I. To create CH_3Cl heteroclusters, CH_3Cl gas was bubbled (at ca. 3.7 atm) through a reservoir containing the oxygen-containing liquid in equilibrium with its vapor at 29 °C. For CH_3I, the liquids were premixed in the reservoir (ca. 1:1 by volume); He (at 3.7 atm.) carrier gas was bubbled through the reservoir.

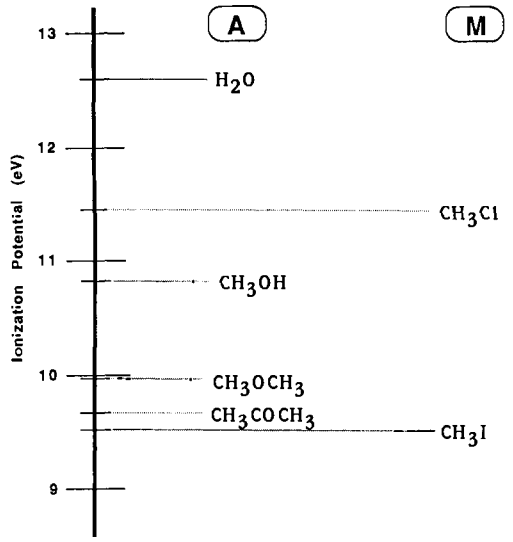

Figure 1. Ionization potentials[59] for relevant molecules.

Table I. Summary of Known Heats of Reaction ($-\Delta H$ in kJ mol^{-1})[a] for Hydrogen

		M		
A	reaction	CH_3Cl	CH_3I	A
H_2O	$M^+ + A$	−50	−176	113
	$A^+ + M$	−188	−184	113
$(CH_3)_2CO$	$M^+ + A$	36	−88	21
	$A^+ + M$	13	4	21
CH_3OH	$M^+ + A$	54 (13)[b]	−71 (−113)[b]	105
	$A^+ + M$	71	63	105
$(CH_3)_2O$	$M^+ + A$	59	−67	59
	$A^+ + M$	26	17	59
homocluster ions	$M^+ + M$	26	−109	

[a] Calculated heats of reaction at ca. 298 K based on ref 32, 41, 42, and 59. [b] Numbers in parentheses refer to cleavage of O–H bond; all other numbers are for C–H bond cleavage.

for via a proposed reaction scheme. Each scheme attempts to depict how the observed product ions are derived from the cluster ions formed by the initial EI step. The equations shown within boxes are provided as heuristic aids to suggest plausible "transition states" which could form the observed product ion.

The use of perdeuteriated analogues of several of the oxy molecules has allowed us to trace the various ion–molecule reactions within the heterocluster. In all the cases studied we observe no evidence for H/D scrambling within the mass spectrum (i.e., there are no progressions of peaks which would result from H's and D's scrambled in the cluster). Rather, we observe that the H's and D's remain intact on their original M or A. This is a common feature of most exothermic ion–molecule reactions, implying that the reactive intermediate formed does not have sufficient energy or lifetime for isotopic scrambling to occur. Therefore the observation of $M_nA_mH^+$ vs. $M_nA_mD^+$, for these systems, is a reliable indication of competing (branching) reactions within the heterocluster.

For each heterosystem it is assumed that the *ion* within the cluster is that of the molecule with the lowest ionization potential (IP). This is reasonable since rapid electronic energy transfer can occur within the cluster. This effect has been recently experimentally observed by Kampe and co-workers,[38] for benzonitrile–rare gas clusters, and has been termed "intramolecular Penning ionization".

This effect, i.e., the net positive charge in the heterocluster ion being localized on the molecule of lowest IP, has also been justified by Grover and co-workers[39] via a qualitative molecular orbital argument. We have made this assumption (as well as in a previous publication[40]) in all cases except those where the IPs of A and M differ by less than 1.0 eV. In such a case we consider the possibility that either or both molecular species may be ionized. However, the assumption appears to be valid in every case, as will be shown below.

Scheme I

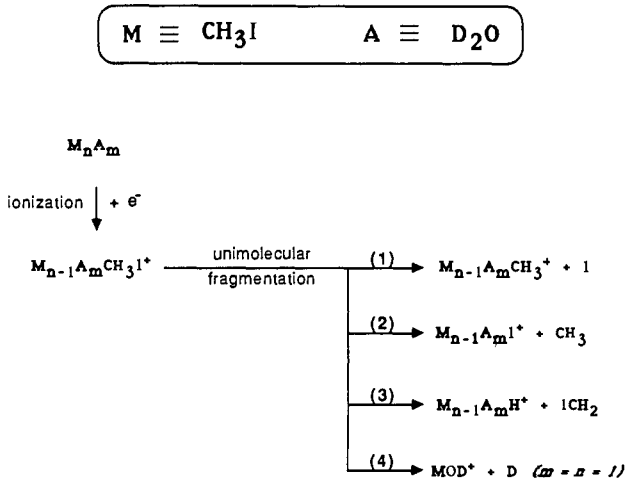

Figure 1 depicts the IPs of all relevant molecules.

(a) Methyl Iodide–Water. Table I lists the heats of reaction for all systems discussed in this paper. These numbers are based on known proton affinities and bond energies.[41,42]

Figures 2 and 3 show typical mass spectra for CH_3I–H_2O and CH_3I–D_2O. For the trivial reason that the CH_3I vapor pressure is much greater than that of the water, and thus the composition of the neutral cluster is excess in CH_3I, the methyl iodide derived peaks dominate the spectra. Those peaks which are unambiguously due to heteroclusters are marked by arrows. The processes which account for them are summarized in Scheme I. Assuming (on the basis of the IP considerations as noted above) that the ion in the heterocluster is that of CH_3I^+, we see that all the peaks can be accounted for by unimolecular fragmentation of the excited ion (with no need to invoke any ion–molecule reactive mechanism).

From Table I we see that hydrogen transfer to a CH_3I ion from either a neutral water molecule or another CH_3I molecule is highly endothermic, and the reaction will not occur.

The major processes which do occur are those denoted I-1 and I-2, involving fragmentation of the C–I bond. An order of magnitude less important are processes I-3 (fragmentation of the C–H bond) and I-4 (fragmentation of the O–H or O–D bond). For I-4 to occur it would be necessary for energy to be transferred from the excited CH_3I^+ to a neutral water molecule, which could then fragment. Because of the energy-transfer requirement, this process, as well as all other fragmentation processes, is expected to become less and less probable for larger clusters since any excess excitation energy will now be distributed over many more vibrational modes of the cluster ion, thereby making localization of that energy into the fissile bond much less probable. This effect, i.e., unimolecular fragmentation becoming less likely for larger cluster ions, is observed for the case of neat $(CH_3)_2O$ clusters (see section 3g).

(b) Methyl Chloride–Water. Figures 4 and 5 show typical mass spectra for CH_3Cl–H_2O and CH_3Cl–D_2O. The composition of the neutral cluster is excess in CH_3Cl. Peaks which have previously been observed with neat CH_3Cl clusters[29] are identified with dots over the respective peaks. Those peaks which result from ionization of the heterocluster (marked by arrows) are correlated via the connection diagram beneath the mass spectra. The processes which account for these peaks are summarized in Scheme II.

(38) Kamke, W.; Kamke, B.; Kiefl, H. U.; Hertel, I. V. *Chem. Phys. Lett.* **1985**, *122*, 356.
(39) Grover, J. R.; Walters, E. A.; Newman, J. K.; White, M. G. *J. Am. Chem. Soc.* **1985**, *107*, 7329.
(40) Garvey, J. F.; Bernstein, R. B. *J. Am. Chem. Soc.* **1986**, *108*, 6096. Erratum: The indices *n* and *m* were used interchangeably for describing neat clusters. In this paper the index *n* is used for methyl halides (M) while *m* is reserved for the oxy compound (A).
(41) Kebarle, P. *Annu. Rev. Phys. Chem.* **1977**, *27*, 445.
(42) *JANAF Thermochemical Tables*, U.S. Dept. of Commerce, NSRDS-NBS537.

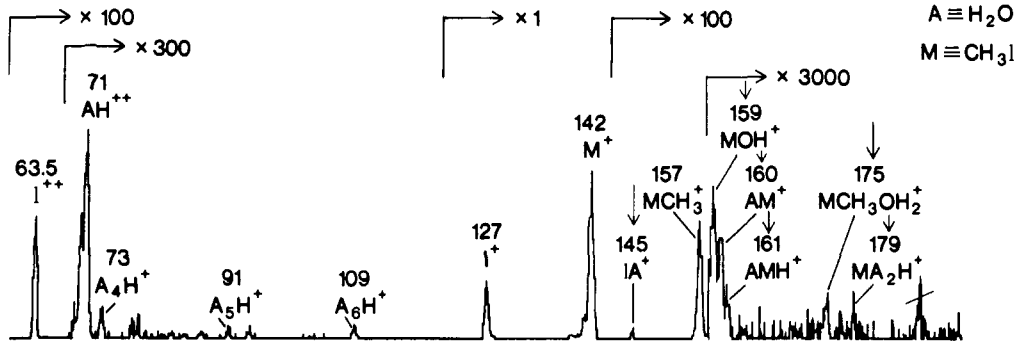

Figure 2. Typical EI (70-eV) mass spectrum of a $(CH_3I)_n(H_2O)_m$ cluster beam. Mass assignments and empirical formulas are indicated for each major ion peak. Relative sensitivity factors appear at the top. A slash mark through a peak denotes a known impurity. Arrows above the mass spectrum indicate an ion peak which must originate from a heterocluster.

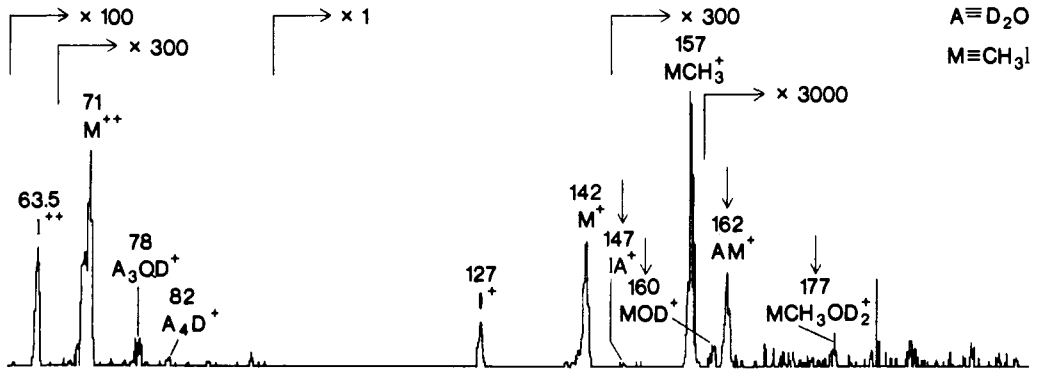

Figure 3. Typical mass spectrum of a $(CH_3I)_n(D_2O)_m$ cluster beam. Presentation as in Figure 2.

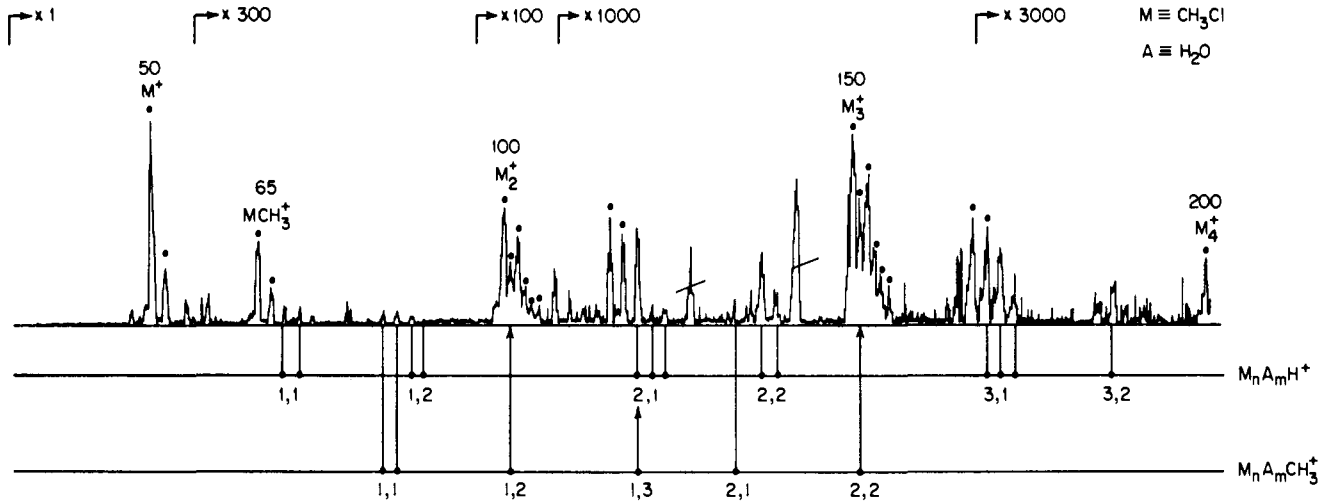

Figure 4. Typical EI (70-eV) mass spectrum of a $(CH_3Cl)_n(H_2O)_m$ cluster beam. Mass assignments and empirical formulas are indicated for each major ion peak. For isotopic peaks that appear together as a clump, only the most intense peak (i.e., for all ^{35}Cl isotopes) is identified. Peaks denoted by a dot are those that also appear in neat CH_3Cl expansions. The numbers denoted n or n,m under the peaks identify the empirical formula of the ion. Relative sensitivity factors appear at the top. A slash mark through a peak denotes a known impurity. Arrows below the mass spectrum indicate dual assignment of a mass peak.

It is interesting to note that the $(CH_3)_2Cl^+$ produced (II-2 and II-4) should methylate H_2O to give $CH_3OH_2^+$ which then should subsequently undergo HCl elimination with CH_3Cl to yield $(CH_3)_2OH^+$ and $(CH_3)_3O^+$. The total absence of these peaks suggests that these processes do not occur within the heterocluster.

Assuming (as usual) that the initial ion is that of CH_3Cl, we see that all the peaks can be accounted for by an ion–molecule reactive mechanism. The major processes are II-1 and II-3, which involve the abstraction of a hydrogen (or deuterium) by the CH_3Cl^+ from a CH_3Cl neutral (or from neutral D_2O). For these processes $-\Delta H^{rxn} = 26$ and -50 kJ mol^{-1}, respectively. (Apparently, endothermicities up to ca. 50 kJ mol^{-1} *can* be overcome when the ion is generated by 70-eV electrons, but the exothermic processes dominate.) This newly generated protonated cluster can then undergo a second reaction, II-2 and II-4, which involves elimination of a neutral HCl (or DCl). The product ion remaining from process II-2 and II-4 is indistinguishable from the ion from unimolecular fragmentation of the C–Cl bond. However, on the basis of several considerations, it is believed that fragmentation does not compete effectively with these fast ion–molecule reactions. This is borne out with the methanol system (see section 3e).

Because of the small mass of H_2O, we are able to observe a relatively large range of cluster sizes and thus a large number of cluster products resulting from these reactions. By measuring the intensities of these various product ions we are able to estimate certain key "branching ratios" as a function of cluster size. We are also able to determine the relative efficiency of reaction II-1 vs. II-3 and ascertain how these relative rate constants vary as a function of cluster size. These results will be presented and discussed in section 4.

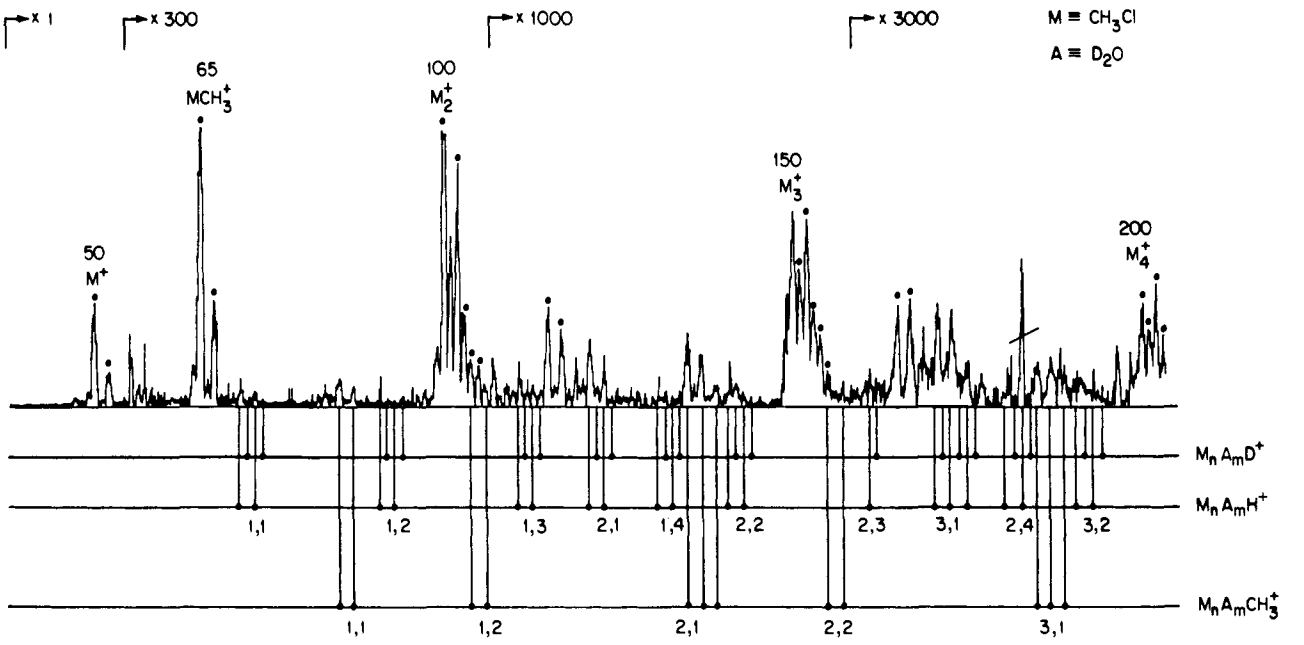

Figure 5. Typical mass spectrum of a $(CH_3Cl)_n(D_2O)_m$ cluster beam. Presentation as in Figure 4.

Scheme II

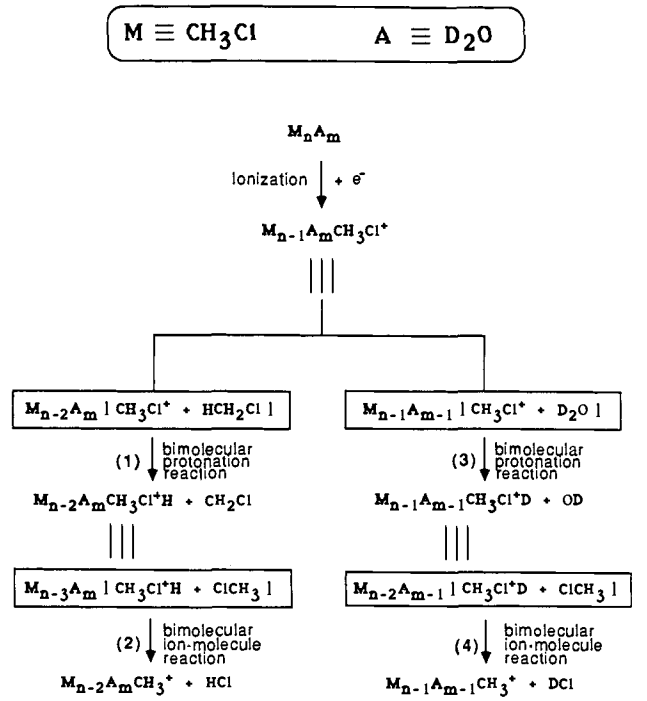

Scheme III

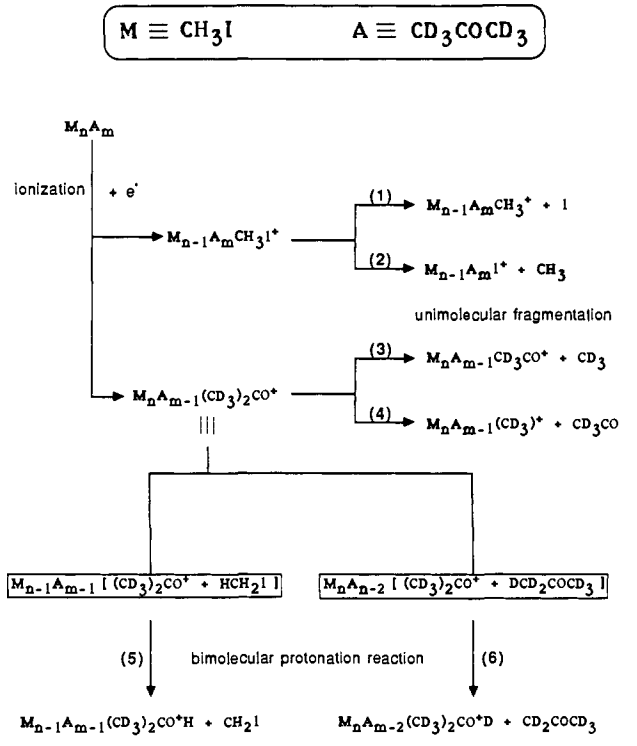

(c) Methyl Iodide–Acetone. Figures 6 and 7 show typical mass spectra for CH_3I–$(CH_3)_2CO$ and CH_3I–$(CD_3)_2CO$. For these systems acetone ion and CH_3I^+ peaks have similar intensities (indicating that the composition of the clusters is roughly equal in concentration of both species). Peaks marked by arrows indicate ions which are unambiguously due to heteroclusters. Since the IPs of both molecules are close (see Figure 2), we must assume that both types of ions are produced initially. Scheme III summarizes the processes.

As in the case of water, when the CH_3I^+ is generated it can only undergo unimolecular fragmentation (hydrogen transfer from neutral acetone is endothermic by 88 kJ mol^{-1}). As a result, an important process is cleavage of the C–I bond (III-1 and III-2). However, an acetone ion can also apparently be generated initially. When it is associated with CH_3I it can either fragment or react. For this system fragmentation involves the endothermic cleavage of a C–C bond (III-3 and III-4) and is only a minor process. The major processes are the exothermic abstractions by the acetone ion of either a hydrogen from a CH_3I (III-5), exothermic by 4 kJ mol^{-1}, or of a deuterium from a neutral acetone (III-6), exothermic by 21 kJ mol^{-1}. However, because of the large masses of these clusters, our data base is limited to the smaller clusters only. Thus we are unable to do the type of analysis of section 3b.

(d) Methyl Chloride–Acetone. The mass spectra for this system have been published,[40] and the scheme is presented here only for the sake of completeness (Scheme IV).

As before, because of IP considerations, the acetone ion is initially generated within the methyl chloride–acetone heterocluster. Once formed the ion can abstract a hydrogen either from a CH_3Cl (IV-1, exothermic by 36 kJ mol^{-1}) or from another neutral acetone molecule (IV-4, exothermic by 21 kJ mol^{-1}). By the use of perdeuteriated acetone, one can differentiate between the two processes, and relative rate constants can be calculated.

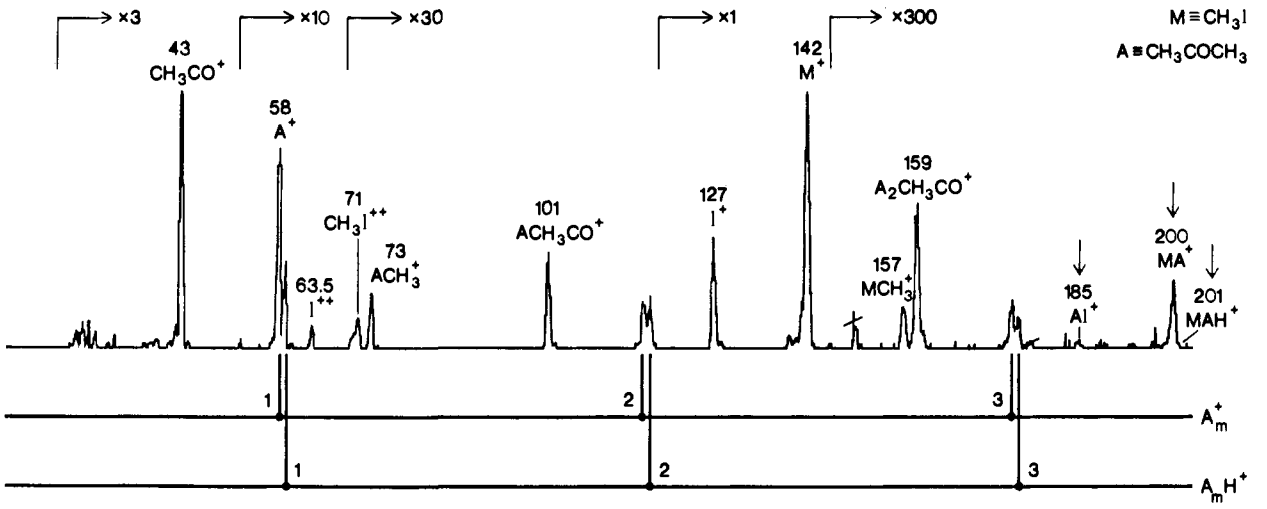

Figure 6. Typical mass spectrum of a $(CH_3I)_n((CH_3)_2CO)_m$ cluster beam. Presentation as in Figure 4.

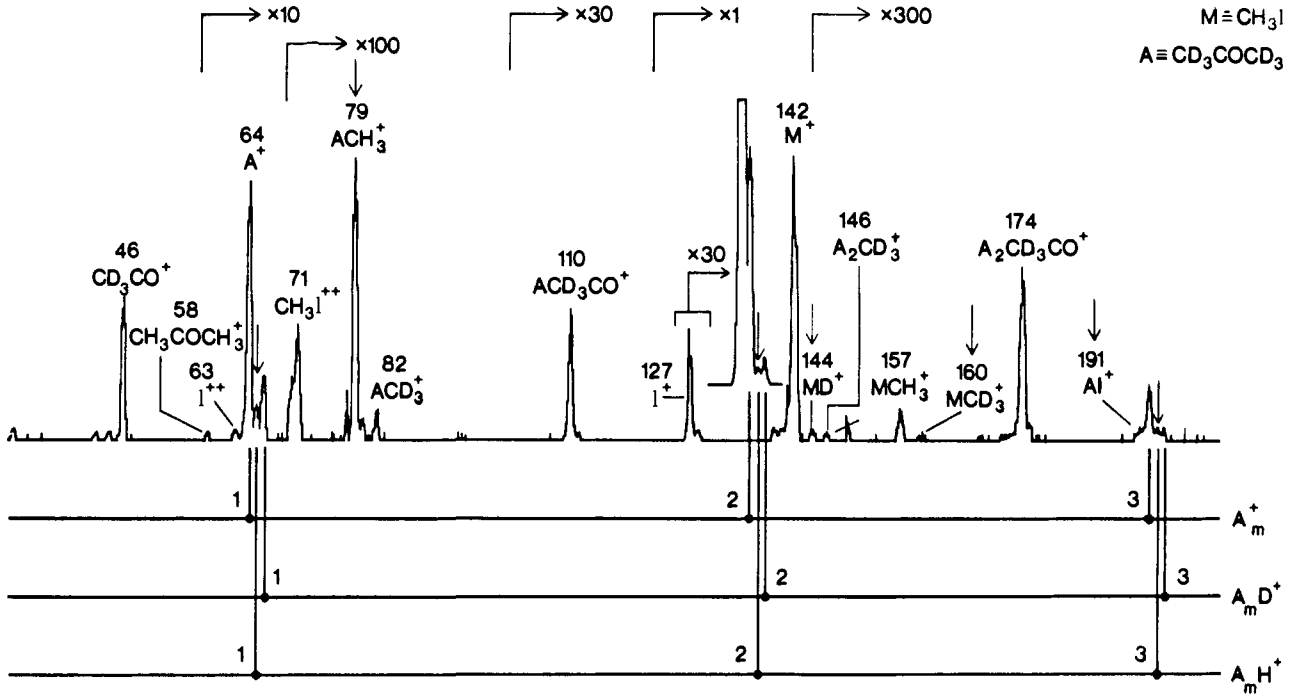

Figure 7. Typical mass spectrum of a $(CH_3I)_n((CD_3)_2CO)_m$ cluster beam. Presentation as in Figure 4.

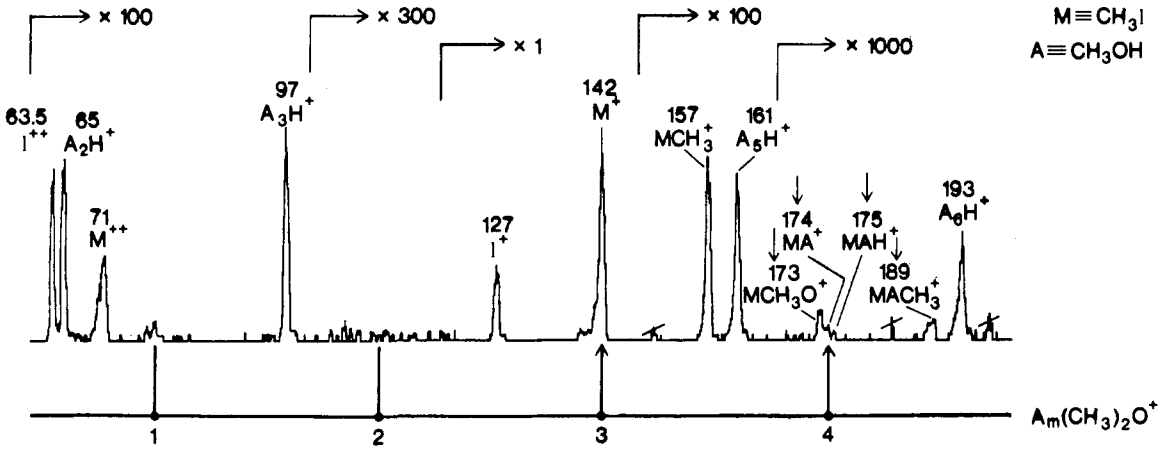

Figure 8. Typical mass spectrum of a $(CH_3I)_n(CH_3OH)_m$ cluster beam. Presentation as in Figure 4.

These are discussed in section 4.

The protonated heterocluster can further react via the exothermic elimination of either HCl or DCl (IV-2 or IV-5) to form a methyl heterocluster ion. This ion could also be formed by fragmentation of the original heterocluster ion, but as shown later, fragmentation does not compete effectively with these fast ion–molecule reactions. A less important reactive (endothermic) pathway leads to elimination of CH_4 or CH_3D (IV-3 or IV-6),

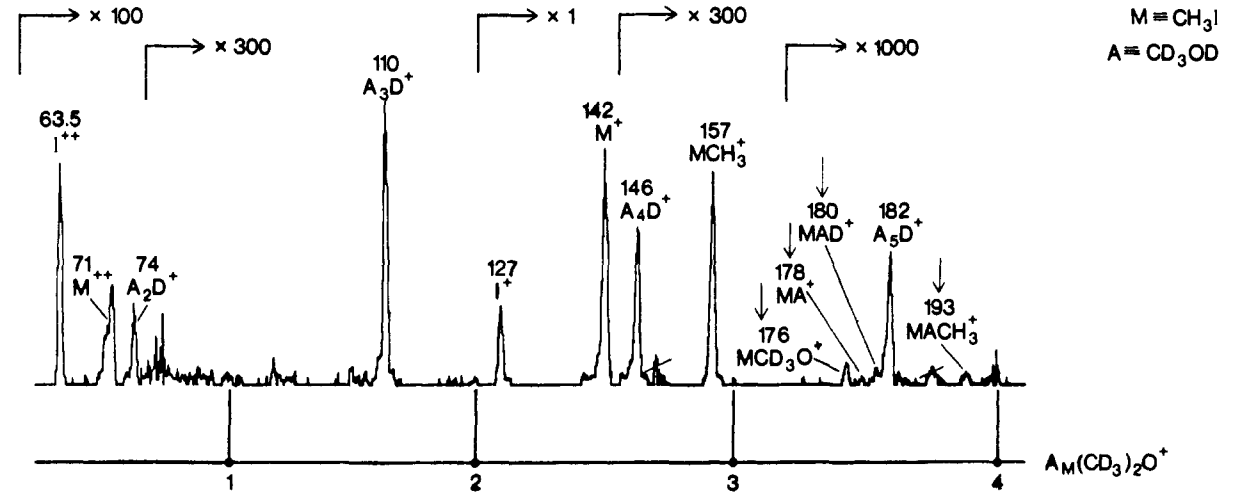

Figure 9. Typical mass spectrum of a $(CH_3I)_n(CD_3OD)_m$ cluster beam. Presentation as in Figure 4.

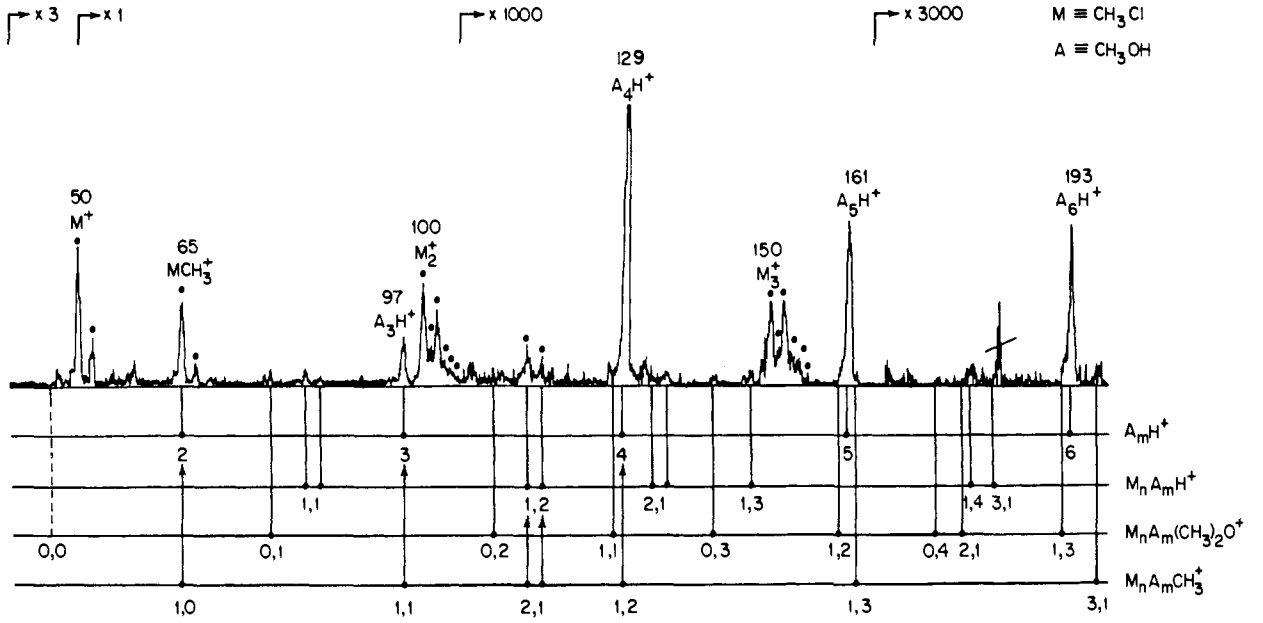

Figure 10. Typical mass spectrum of a $(CH_3Cl)_n(CH_3OH)_m$ cluster beam. Presentation as in Figure 4. Dashed line indicates uncertain assignment.

forming a halonium heterocluster ion.

(e) Methyl Iodide–Methanol. Figures 8 and 9 show typical mass spectra for CH_3I–CH_3OH and CH_3I–CD_3OD. Because of IP considerations, CH_3I^+ will be formed initially within the cluster. As previously seen, CH_3I does not react due to endothermicity as is the case for methanol (the reaction of CH_3I^+ to abstract a hydrogen from a neutral methanol is endothermic by 71 kJ mol^{-1}). This system, just as in the case of CH_3I–H_2O, shows exclusively product ions which can be accounted for on the basis of fragmentations alone. The major process (shown in Scheme V) involves cleavage of the C–I bond to form a methyl heterocluster ion (V-1). The only other process involves cleavage of the O–H bond in the methanol and must occur via an energy-transfer process as outlined in section 3a.

It is noteworthy to observe (from Figures 8 and 9) a minor process, namely, the production of dimethyl ether ion clustered with methanol molecules, produced via a dehydration reaction in the neat methanol ion cluster. This system has been studied in detail by ICR techniques.[43-45] In the gas phase, a protonated methanol ion reacts with a neutral methanol molecule to produce a protonated dimethyl ether ion. In contrast, in the cluster we observe that this dehydration reaction can proceed directly from the ionized methanol to form a solvated dimethyl ether ion.

(f) Methyl Chloride–Methanol. Figures 10 and 11 show typical mass spectra for CH_3Cl–CH_3OH and CH_3Cl–CD_3OD. Because the IPs of the two molecules are close, both may form ions.

Scheme IV

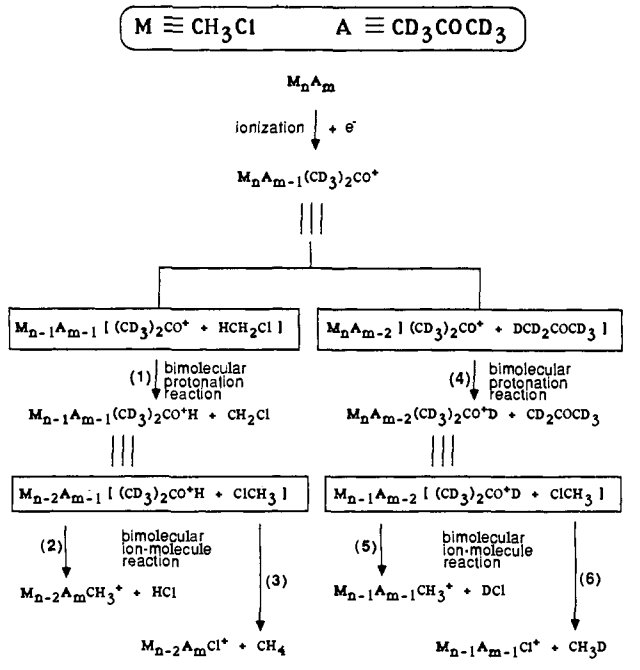

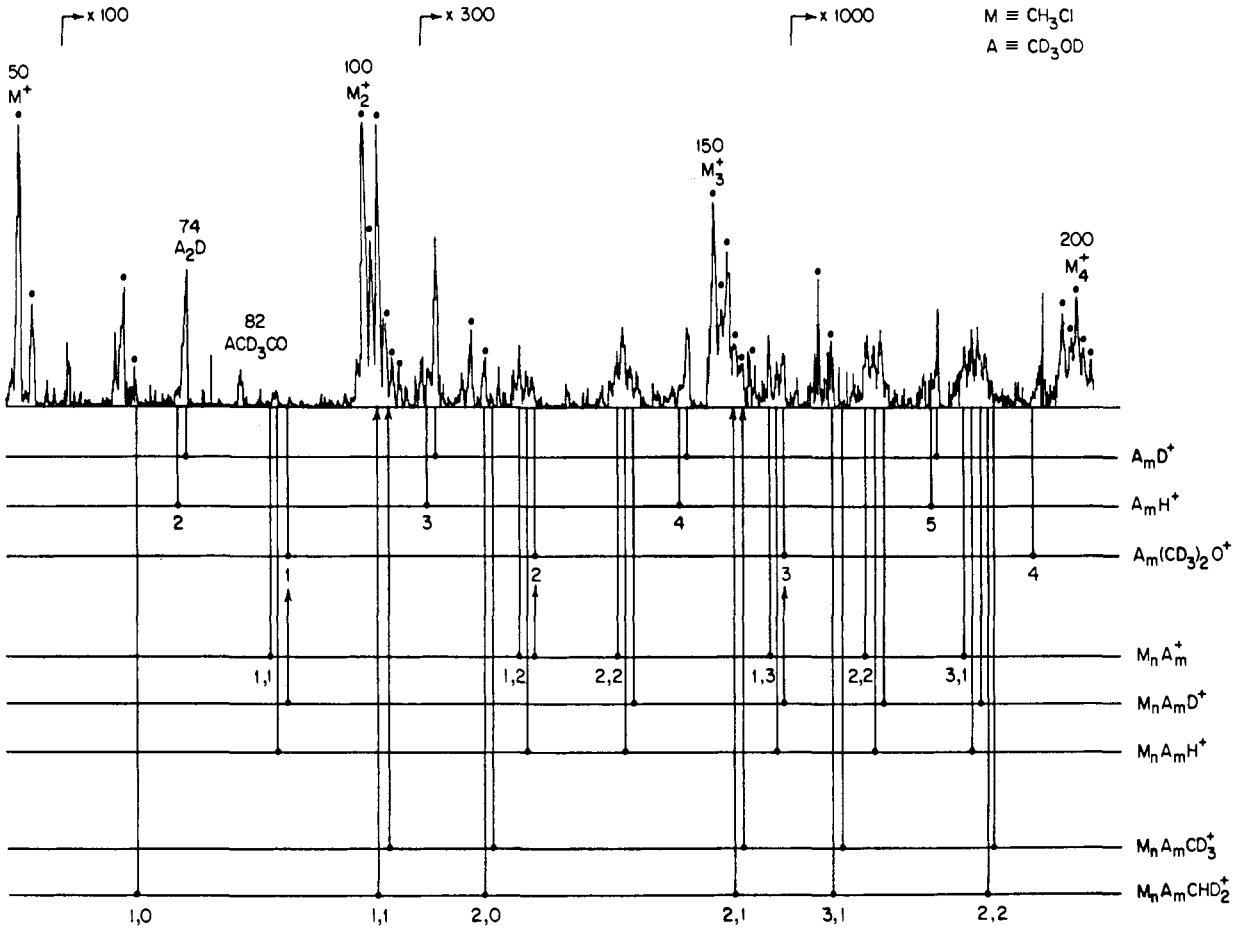

Figure 11. Typical mass spectrum of a $(CH_3Cl)_n(CD_3OD)_m$ cluster beam. Presentation as in Figure 4.

Scheme V

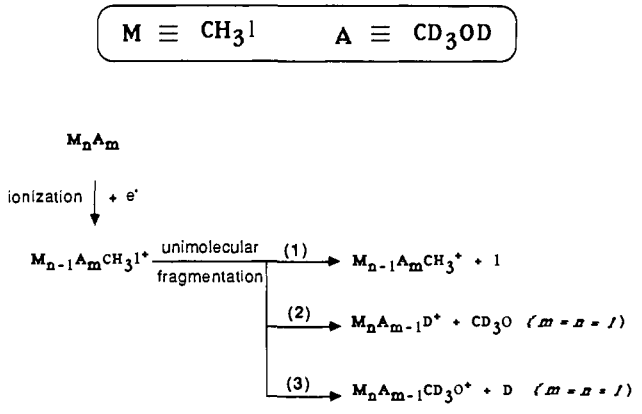

However, there appears to be a preference for the generation of methanol ion. The reactive processes are summarized in Scheme VI.

One again might expect that the $CH_3OH_2^+$ produced (VI-1 and VI-5) could undergo HCl elimination with CH_3Cl to yield $(CH_3)_2OH^+$ and $(CH_3)_3O^+$. However, the total absence of these peaks in the mass spectra (just as in section 3b) suggests that these processes are not occurring within the cluster.

The situation is further complicated by the fact that methanol ion can react with a neutral methanol to dehydrate and form a dimethyl ether ion (VI-4). Due to these complications we are unable to derive relative rate constants (as was possible for the water and acetone systems). Yet, qualitatively, this system shows the same pattern of reactivity as before in that the heterocluster ion rapidly reacts to form a protonated heterocluster ion (VI-1 and VI-5). Once the protonated cluster has been formed it can react by a fast dehydration reaction to form a methyl heterocluster ion (VI-2, VI-3, and VI-4). As before, these methyl heterocluster ions could be formed from unimolecular decay of the heterocluster ion. However, the observed mixed isotopic methyl heterocluster ions (VI-3) could only be produced by this reaction scheme, and not unimolecular fragmentation, showing that fragmentation does not compete with the rapid reaction. As stated above, this process has been studied by ICR techniques.[43-45]

(g) Dimethyl Ether. In this section we report the first observation of an ion–molecule reaction within neat dimethyl ether clusters. Figure 12 is a typical mass spectrum for such a cluster beam. Scheme VII summarizes our observations. We see first that there are no parent cluster peaks observed except for a weak dimer peak. However, protonated dimethyl ether peaks are observed throughout the spectrum. This suggests that the fast hydrogen-transfer reaction (VII-2, exothermic by 59 kJ mol^{-1}) goes to completion for dimethyl ether cluster ions (all the parent cluster ions generated are consumed to form the protonated cluster ions). This is much like the case of neat CH_3F cluster ions[29] where, because of the exothermicity of the reaction (and no barrier to reaction), the process went to completion.

We also observe the generation of clusters corresponding to the loss of methoxy (VII-1). These are probably due to a fragmentation process, cleaving the C–O bond. This is confirmed since these peaks decrease and eventually disappear with cluster size ($n > 2$). As discussed in section 3a, the larger the cluster the more likely the energy is randomized, therefore making fragmentation less likely, with the excess energy being dissipated through rapid chemical reaction (or evaporation).

Further evidence for this cleavage of the C–O bond in ionized dimethyl ether has been recently reported.[46] In this experiment

(43) Henis, J. M. S. *J. Am. Chem. Soc.* **1968**, *90*, 844.
(44) McMahon, T. B.; Beauchamp, J. L. *J. Phys. Chem.* **1977**, *81*, 593.
(45) Bass, L. M.; Cates, R. D.; Jarrold, M. F.; Kirchner, N. J.; Bowers, M. T. *J. Am. Chem. Soc.* **1983**, *105*, 7024.
(46) Eckart, K.; Zummack, W.; Schwarz, H. *Org. Mass Spectrom.* **1984**, *19*, 642.

Scheme VI

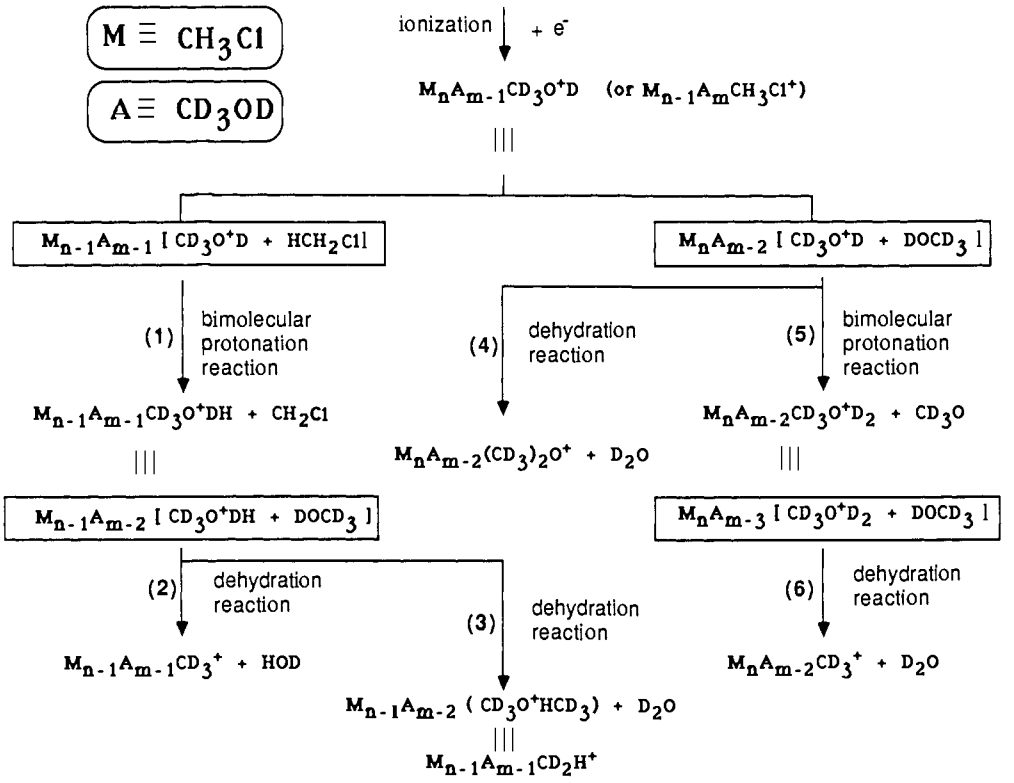

Scheme VII

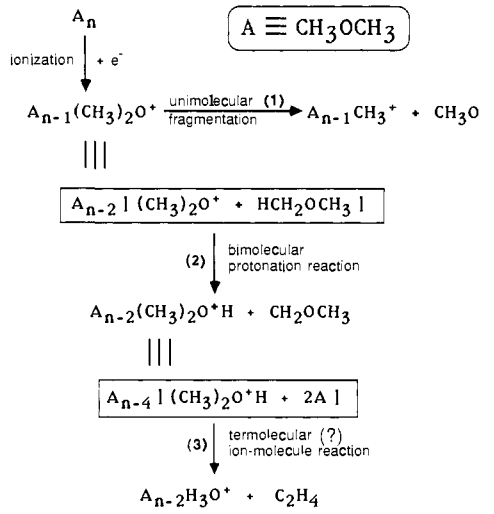

Scheme VIII

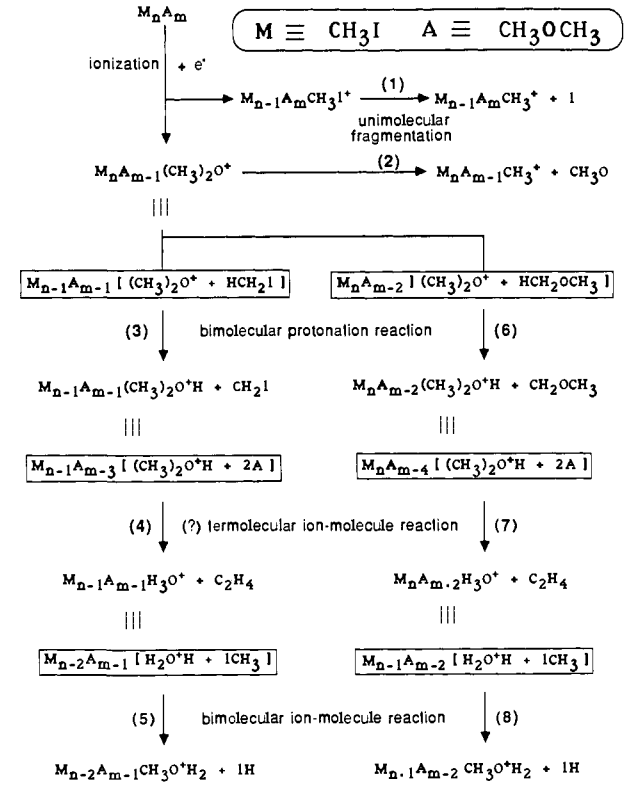

the product is protonated formaldehyde formed via a two-step reaction from the ionized dimethyl ether. However, we do not find this to be an important process for the case of dimethyl ether clusters.

Lastly, we observe the formation of cluster ions of the form $A_n(H_3O)^+$. (This cannot be due to water contamination of the sample since no peak at m/z 18 is observed. Also, these cluster ion peaks are only observed for $n > 1$.) We speculate that these ions are generated via a termolecular process whereby the protonated neat cluster ion of dimethyl ether reacts to eject a C_2H_4 (termolecular since we do not observe the formation of $A(H_3O)^+$ ion which would come from the A_2H^+ precursor).

In a previous paper,[29] we suggested that termolecular processes occurred within neat clusters of CH_3F in order to explain the presence of ion products which had no analogue from bimolecular gas-phase reactions. The observation of this same effect in dimethyl ether suggests that the cluster environment coupled with the magnitude of the exothermicity of the reaction forming the protonated cluster ion determines the likelihood of subsequent endothermic processes occurring within the protonated cluster ion. Whatever the explanation for these new product ions, they result from chemical processes that occur only within the solvated environment of a cluster.

(h) **Methyl Iodide–Dimethyl Ether.** Figure 13 shows typical mass spectra for the CH_3I–$(CH_3)_2O$ system. Scheme VIII summarizes the results for this system. Because of IP considerations, either the CH_3I or the dimethyl ether may ionize within the heterocluster. This does not complicate the chemistry since hy-

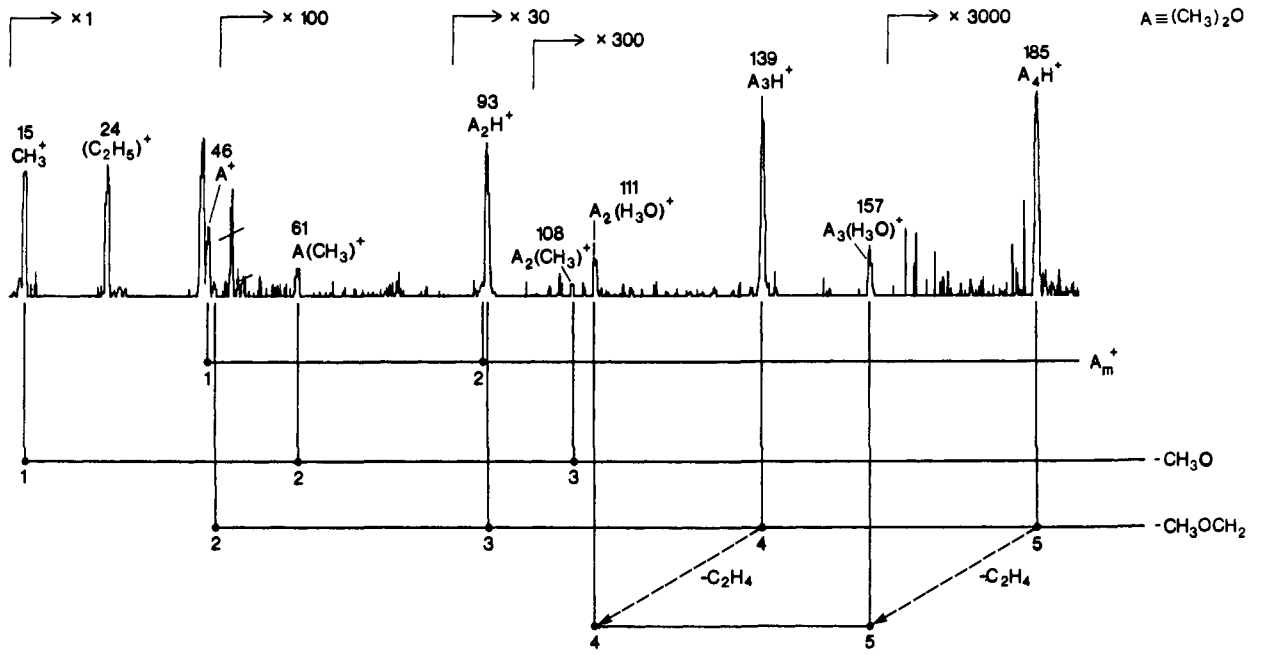

Figure 12. Typical mass spectrum of a $((CH_3)_2O)_m$ cluster beam. Mass assignments and empirical formulas are indicated for each major ion peak. The first set indicates the parent cluster ion with n identifying the empirical formula of the ion. The next line indicates loss of a CH_3O fragment from a parent cluster of size m, where m is the number under the peak. The last two lines indicate subsequent loss of CH_3OCH_2 and then C_2H_4 from a parent cluster of size m, where again m is the number under the peak. Dashed lines represent uncertain processes.

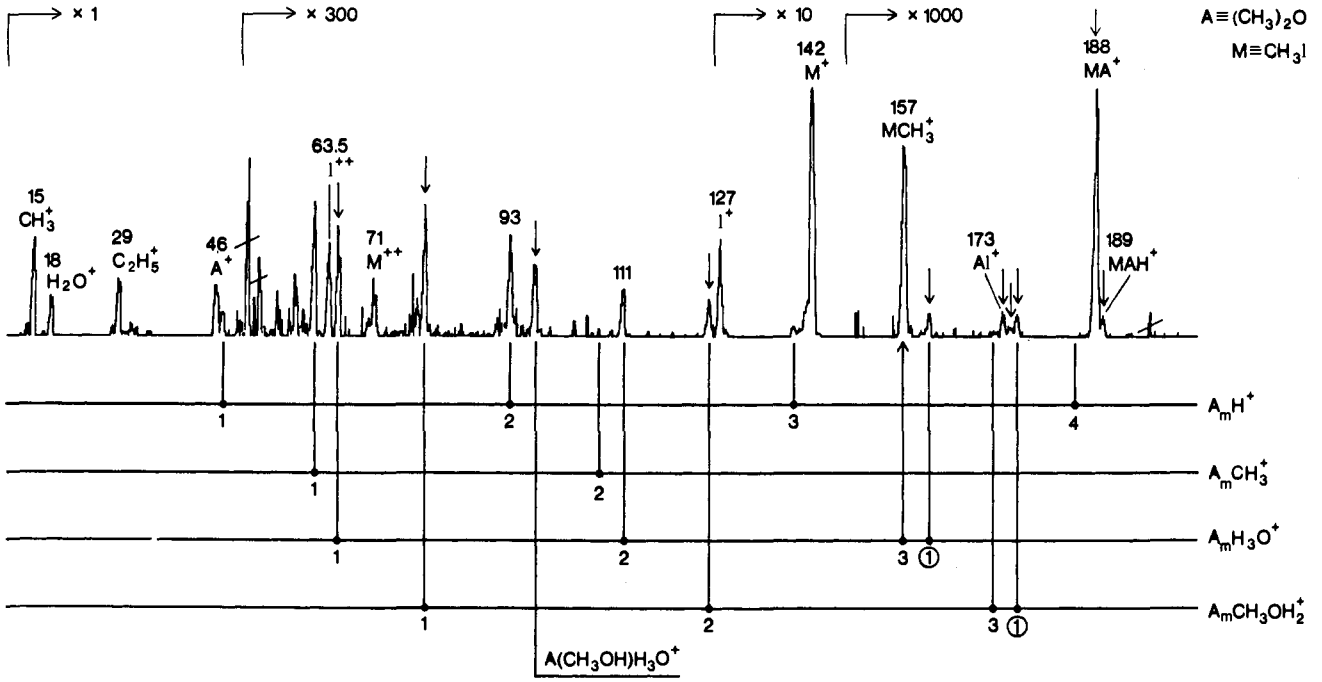

Figure 13. Typical EI mass spectrum of a $(CH_3I)_n((CH_3)_2O)_m$ cluster beam. Mass assignments and empirical formulas are indicated for each major ion peak. The values for m under the peaks identify the empirical formula of the ion. When m is contained in a circle, M is to be substituted for A in the empirical formula of the ion indicated at the right. Arrows below the mass spectrum indicate dual assignment of a mass peak. Arrows above the mass spectrum indicate an ion peak which must originate from a heterocluster.

drogen abstraction by CH_3I^+ from a neutral dimethyl ether is endothermic by 67 kJ mol^{-1}. As a result, the major pathway for CH_3I^+ will be fragmentation (VIII-1), as observed previously for the water and methanol systems.

However, the dimethyl ether ion can abstract a hydrogen either from a neutral CH_3I (VIII-3, exothermic by 17 kJ mol^{-1}) or from a neutral $(CH_3)_2O$ (VIII-6, exothermic by 59 kJ mol^{-1}). Both of these processes effectively compete with unimolecular fragmentation (VIII-2) such that production of the protonated heterocluster is the major process.

Just as in the case of the neat dimethyl ether cluster, the protonated heterocluster can undergo termolecular reactions (VIII-4 and VIII-7), here ejecting an ethylene molecule and leaving an ion of the empirical formula $M_nA_mH_3O^+$.

For the case of neat dimethyl ether cluster ions this would be the end of the reactive scheme, but since this is a heterocluster system, new reactive processes become possible due to the presence of an additional molecule, the methyl halide. One new reaction (VIII-5 and VIII-8) consists of the ejection of neutral HI from the $M_nA_mH_3O^+$ cluster ion producing a product ion of the empirical formula $M_nA_{m-1}(CH_3OH)H^+$. The great reactivity of both neat and heteroclusters of dimethyl ether warrant additional investigation with deuteriated molecules as tracers to ascertain which process dominates. It is clear that the reactivity is due in part to the very stable product ions formed ($M_nA_mH_3O^+$ and $M_nA_{m-1}(CH_3OH)H^+$).

Table II. Relative Reaction Rates as a Function of n and Electron Energy for Hydrogen Transfer to $(CH_3Cl)_n^+$

n	k_n (30 eV)	k_n (70 eV)
2	1.0[a]	1.0[a,b]
3	0.74	0.72
4	0.58	0.63

[a] For convenience the values of k_2 have been set to be unity. [b] Based on the present experiments, the value of k_2 (70 eV) is 1.22 × k_2 (30 eV).

4. Interpretation of Results

In an attempt to understand the dynamics of these ion–molecule reactions within the heteroclusters we shall first deal with the reactions within neat clusters, deriving relative rate constants for several of the processes previously discussed.[28,29]

Consider the case of the neat CH_3Cl clusters. Defining R_n as the ratio of the ion intensity of the protonated $(n-1)$ ion peak to that of the precursor (n) ion peak and assuming a first-order decay process with a rate constant k_n, it can be shown that

$$k_n = t_n^{-1} \ln (R_n + 1) \quad (1)$$

where t_n is the effective time for reaction, i.e., the residence time for the cluster ions in the ionizer of the mass spectrometer before injection into the quadrupole. Although we can only estimate t_n (in the μs range), it has been implicitly assumed to be the same for the various precursor ions being compared.[47]

Our analysis assumes that little or no evaporation occurs from the precursor ion and that the major source of depletion of the cluster ion is via the ion–molecule reaction. Some justification of this assumption has been previously presented.[29] Empirical pressure dependences of CH_3F cluster ions show the same dependence as the protonated product ions.[29] It is shown below that for small clusters, at least, it is almost always the case that the energy barrier for reaction is less than that for evaporation.

We can now apply eq 1 to previous data for $(CH_3Cl)_n$[29] and derive relative rate constants for the protonation reaction as a function of cluster size (and EI electron energy). Results are presented in Table II. The rate constants decrease as the cluster size increases (and as the electron energy is decreased). This is consistent with our previous observation that there appears to be a barrier to this reaction within the cluster.

This is not the case for the CH_3F cluster ions, which protonate to completion, consuming the precursor. (This is also the case for neat water clusters.[48-50]) However, ICR results indicate that the (bimolecular) rates of reaction for CH_3F and CH_3Cl are identical. Why then should there be a barrier to the reaction within the cluster for CH_3Cl and not for CH_3F?

Figure 14 shows the heats of formation for the methyl fluoride, chloride, and bromide systems relative to the protonation products and to dissociation. Examination of the diagram shows that the origin of the barrier to reaction within CH_3Cl clusters lies in the stability of the cluster ion formed. In the case of CH_3F, even though the dimer ion is 48 kJ mol^{-1} stable with respect to dissociation[35] the exothermicity of the reaction (104 kJ mol^{-1}) overcomes it, such that there is no barrier to reaction whether in the cluster or gas phase.

However, for CH_3Cl the reaction is less exothermic ($-\Delta H$ = 26 kJ mol^{-1}), such that the stability of the dimer ion gives rise to a barrier of 22 kJ mol^{-1} (in addition to any intrinsic reaction barrier), which must be overcome to produce the protonated cluster. This barrier is absent in the gas phase. Lastly, for the case of CH_3Br clusters, the reaction is so endothermic that it does not occur in either the gas phase or the cluster.

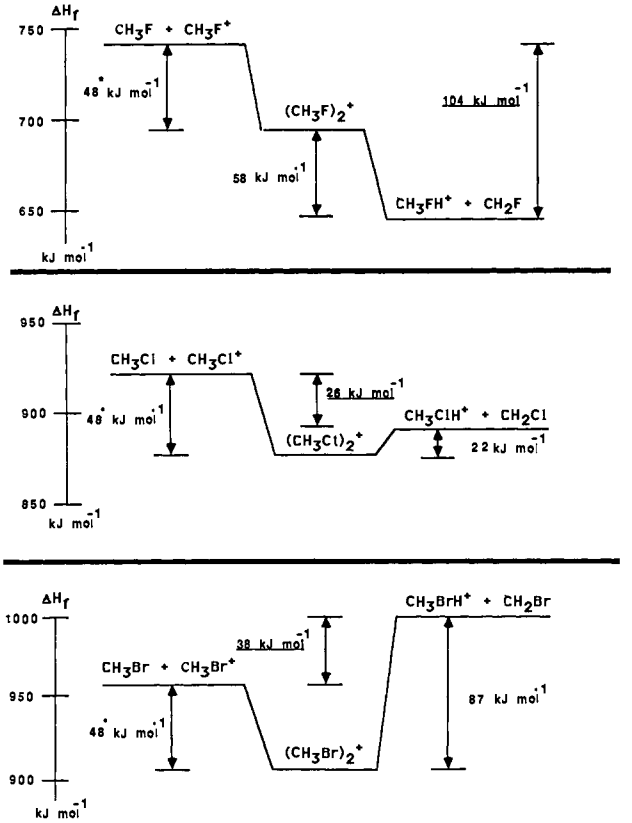

Figure 14. Enthalpy diagram for dimer ions of methyl halides relative to dissociation of the dimer or hydrogen transfer. The heats of formation of the separate ion and molecule are calculated from thermodynamic data,[41,42] while the shaded arrows are calculated from IPs[59] and ICR results.[32] The energy of the CH_3F dimer ion (as denoted by *) was taken from ref 35 and is assumed to be the same for the other methyl halide dimer ions.

Table III. Relative Rates of Reaction for Acetone–Methyl Chloride

m	$(MA_{m-1})^+ \rightarrow (A_{m-1}H)^+$ k_{rel}(IV-1)	$(A_m)^+ \rightarrow (A_{m-1}D)^+$ k_{rel}(IV-4)	$\frac{k(\text{IV-1})}{k(\text{IV-4})}$
2	1.0[a]	1.0[a]	4.3
3	1.2	0.7	7.2

[a] $(k_{rel})_2$ set at unity.

As a result, we now can explain the data of Table II. Reaction rate increases as electron energy increases since the additional internal energy helps overcome the barrier to the protonation reaction in the cluster ion case. Increasing cluster size decreases the reaction rate since the larger the cluster the more the internal energy will be randomized, with less available for overcoming the barrier. Note that for both CH_3Cl and CH_3F the barrier to reaction is substantially less than that for evaporation.

We see then that the overall dynamics of these neat cluster ion–molecule reactions depend on (a) the overall energetics of the gas-phase reaction and (b) the stability of the ion cluster initially produced. The more exothermic the reaction and the less stable the ion cluster precursor, the more rapid the ion–molecule reaction.

We can now take these qualitative observations for neat methyl halide clusters and see how they apply to the heteroclusters. Consider first the CH_3Cl–$(CH_3)_2CO$ system for which we contrast the neat cluster reaction with heterocluster reactions. Table III presents the relevant relative rate constants.

Figure 15 shows heats of formation for various acetone cluster ions relative to dissociation and reaction. We see that for small clusters the reaction competes energetically with evaporation and that, just as in the neat CH_3Cl case, the stability of the acetone dimer ion gives rise to a barrier to reaction (20 kJ mol^{-1}).

(47) For our mass range, the residence time of the heaviest ion (m/z 200) in the ionizer is ca. a factor of 2 greater than that of the lighest ion (m/z 50). It should also be noted that the microchannel plate (ion–electron multiplier) in the detector exhibits a mass-weighed bias such that higher mass intensity will be detected with less efficiency (roughly a factor of 5). Thus only qualitative information on relative yields of different cluster ions can be obtained from the present experiment.

(48) Kebarle, P. K.; Searles, S. K.; Zolia, A.; Scarborough, I.; Arshdi, M. *J. Am. Chem. Soc.* **1967**, *89*, 6393.
(49) Searcy, J. Q.; Fenn, J. B. *J. Chem. Phys.* **1974**, *61*, 5282.
(50) Bohme, D. K.; Mackay, G. I.; Tanner, S. D. *J. Am. Chem. Soc.* **1979**, *101*, 3724.

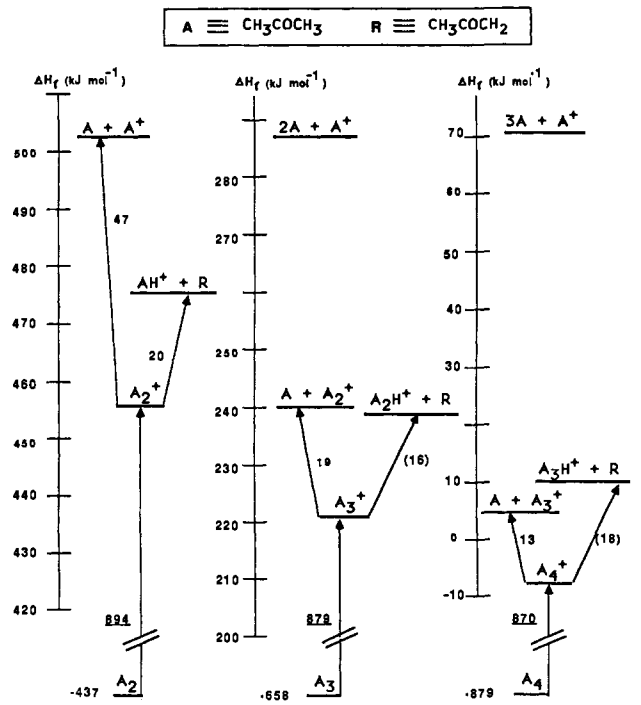

Figure 15. Energy level diagram of acetone cluster ions. Underlined values were obtained from photoionization data,[59] other values from thermochemical data.[41,42,60] Numbers in parentheses calculated with the assumption that the proton affinity of A_m^+ is the same as that of A^+.

The only approximation made in constructing Figure 15 is that the hydrogen affinity of any size acetone cluster ion is equivalent to that of the "bare" acetone ion. From this assumption it appears that the barrier to reaction will be approximately constant as a function of m and that relative rates should be the same. Table III shows that rate constants decrease with cluster size, which in turn suggests that hydrogen affinities decrease as the cluster ion size increases. This effect has been observed in the case of HF clusters.[51]

For the heterocluster ions we can see from Table III that abstraction of a hydrogen by the acetone ion from a CH_3Cl in a heterocluster is much more probable than abstraction from a neutral acetone molecule within a neat cluster. This is at first surprising since both bimolecular reactions are exothermic, with abstraction from a neutral acetone molecule being *more* exothermic by some 8 kJ mol^{-1}. Why then should the reaction within a heterocluster be faster than in a neat cluster?

A possible explanation for this (when the gas-phase reaction energetics suggest they should be similar) lies in the fact that a heterocluster ion is inherently less stable then a neat cluster ion. That is, if the ΔH_f of MA^+ is greater that of A_2^+ (457 kJ mol^{-1}), then the barrier to reaction will be less and the reaction rate faster.

It has been observed by many workers[35,39,52-57] that homodimer ions are usually more stable than "corresponding" heterodimer ions. This is experimentally determined by observing that the threshold cross section for the production of the monomer ion by dissociative photoionization is usually much greater for the heterodimer than for the homodimer. Grover and co-workers[39] have suggested that since the valence orbitals of the heterodimer ions are unequal in energy, this means less interaction (according to standard MO theory) and therefore less stability.

Thus it appears that all heterocluster ion–molecule reactions should be faster than corresponding neat cluster ion–molecule reactions and that the difference in reactivity is related to the differences in IPs of the separated molecules which comprise the heterocluster. The larger the difference, the less stable will be the heterocluster ion and therefore the greater the reactivity.

For the CH_3Cl–water system the relative rates increase with cluster size (Table IV). This trend is opposite to that observed for neat CH_3Cl clusters.[29] It is tempting to suggest that this is another intrinsic difference between neat cluster ions and heterocluster ions: as the heterocluster ions become larger they become less stable compared to the corresponding neat cluster of similar size. There appear to be no photoionization data available for heteroclusters as a function of size; such measurements would greatly help in clarifying this point.

Thus far we have discussed only clusters in which the initially formed ion could abstract a hydrogen only from *one* other type of molecule. However, for heteroclusters competitive (branching) reactions are possible; M^+ in $M^+(M_{n-1}A_m)$ can abstract a hydrogen from M with rate constant $k_{n,m}$ and a deuterium from A with rate constant $k'_{n,m}$. Assuming first-order kinetics, it can be shown that the branching ratio, say $B_{n,m}$, namely, the ratio of ion intensity of the protonated cluster ion product to that of the deuteriated cluster ion, is given by $B_{n,m} = k_{n,m}/k'_{n,m}$. Figures 16–19 report such experimental branching ratios for both the CH_3Cl–acetone and CH_3Cl–water systems.

For each set of data we assume the first entry in the figure to be the "reference set". The analysis shows that as we increase the concentration of either reagent in the cluster, that is M or A, the branching ratio behaves in a purely statistical fashion[58]

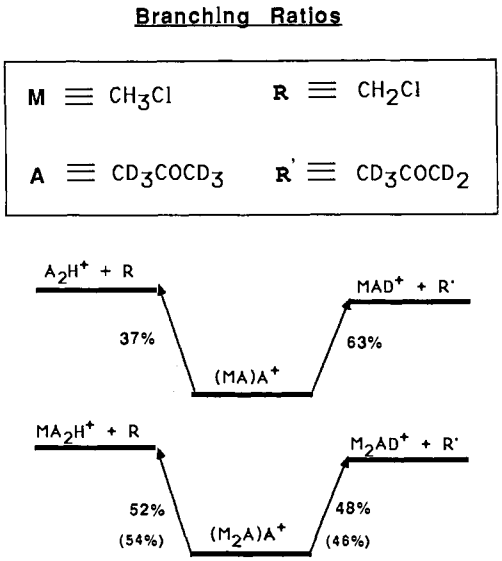

Figure 16. Branching ratio for the CH_3Cl–$(CD_3)_2CO$ system. Numbers in parentheses represent statistical predictions[58] based on the uppermost entry in the figure. Placement of the product energy levels relative to the precursor level serves as a heuristic aid.

Table IV. Relative Rates of Reaction for Water–Methyl Chloride

m	$(MA_m)^+ \rightarrow (MA_{m-1}D)^+$ k_{rel}(II-3)
2	1.0[a]
3	2.8
4	5.3

[a] $(k_{rel})_2$ set at unity.

(51) Tiedemann, P. W.; Lee, Y. T. *An. Conf. Fis.-Quim. Org., 1st* **1982**, 204.
(52) Tiedemann, P. W.; Anderson, S. L.; Ceyer, S. T.; Hirooka, T.; Ng, C. Y.; Mahan, B. H.; Lee, Y. T. *J. Chem. Phys.* **1979**, *71*, 605.
(53) Ono, Y.; Osuch, E. A.; Ng, C. Y. *J. Phys. Chem.* **1981**, *74*, 1645.
(54) Pratt, S. T.; Dehmer, P. M. *J. Chem. Phys.* **1983**, *77*, 6336.
(55) Meot-Ner, M. *Acc. Chem. Res.* **1984**, *17*, 186.
(56) Walters, E. A.; Grover, J. R.; White, M. G.; Hui, E. T. *J. Phys. Chem.* **1985**, *89*, 3814.
(57) Ruhl, E.; Bisling, P. G. F.; Brutschy, B.; Baumgärtel, H. *Chem. Phys. Lett.* **1986**, *126*, 232.

(58) From the first entry in Figure 17 we can say for the $M^+(MA)$ precursor that CH_3ClH^+ preferentially abstracts a hydrogen from an M vs. an A by a 4:1 ratio. Using this as a reference, we now consider a $M^+(MA_2)$ precursor, for which the neutral A concentration has been doubled. If the reaction efficiency is purely dependent on the amount of reagent present, then the branching ratio should now be 4:2. In this way statistical predictions can be made. They are seen to agree well with the data.

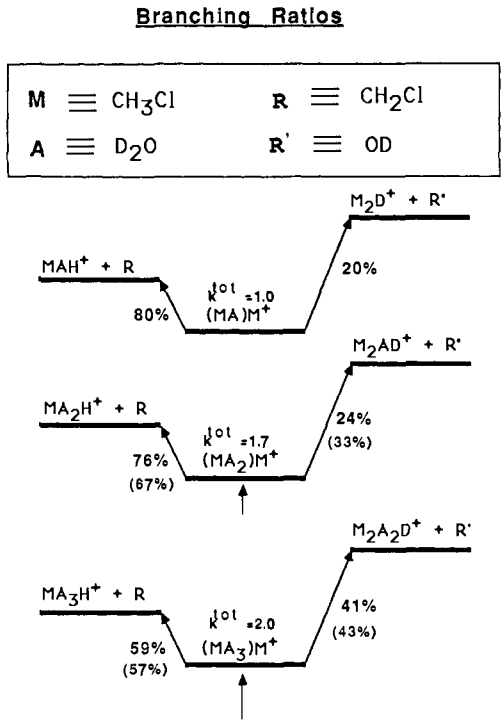

Figure 17. Branching ratio for CH_3Cl–D_2O system, as a function of the molar ratio of D_2O in the precursor. Numbers in parentheses represent statistical predictions.[58] As in Figure 16, these are based on the uppermost entries in the figure. Placement of the product energy levels relative to the precursor level is qualitative and serves purely as a heuristic aid. Relative total rate constants k^{tot} relative to that for $(MA)M^+$ are listed. Arrows underneath the precursor indicate how the energy level must be shifted in order to compensate qualitatively for the deviations from statistical behavior.

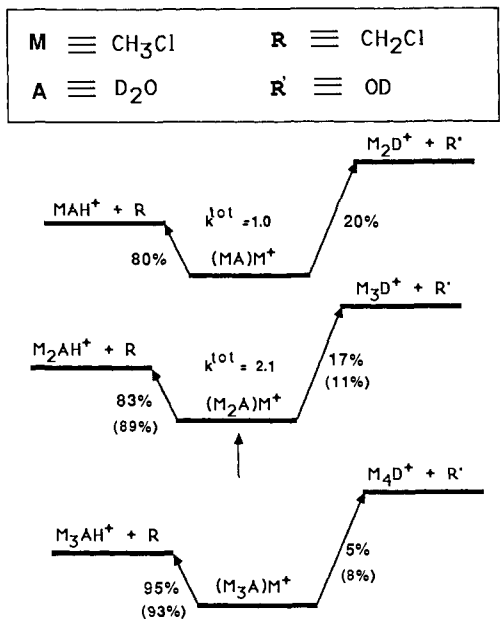

Figure 18. Branching ratio for the CH_3Cl–D_2O system as the concentration of CH_3Cl increases. See caption for Figure 17.

as a function of the M/A ratio, i.e., it increases in a linear way with respect to the increase of one of the reagents. This suggests that the differences between the energy levels of the protonated and deuteriated cluster product ion do not change a great deal as a function of cluster size.

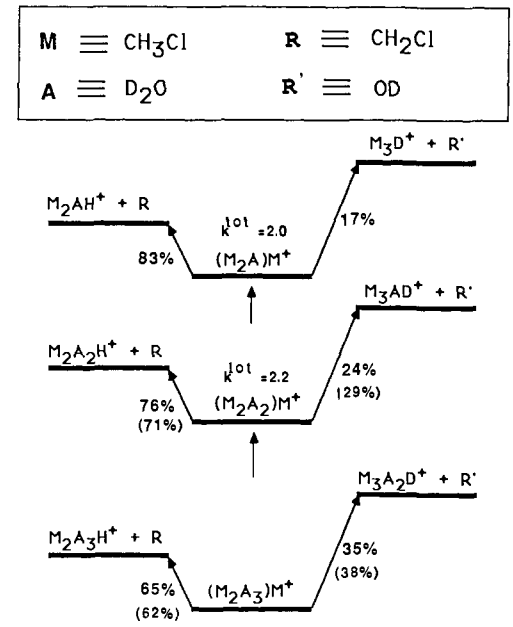

Figure 19. Branching ratio for the CH_3Cl–D_2O system as the concentration of D_2O increases. See caption for Figure 17.

For the methyl chloride–water system we are able to calculate k^{tot} from eq 1 (where $k^{tot} = k_{n,m} + k'_{n,m}$ and $t_{n,m}$ is assumed to be independent of n and m) by defining R now to be the ratio of the sum of the ion intensities of the protonated $(n-1, m)$ and deuteriated $(n, m-1)$ ion peaks to that of the precursor (n, m) ion peak. Figures 17–19 list the relative values for k^{tot} for the CH_3Cl–water system. In every case, as with the CH_3Cl–acetone system, the larger the cluster the faster the rate. Since the product branching ratios appear to be consistent with a statistical interpretation, this difference in the total rate must be due to a difference in the stability of the heterocluster precursor ion which is initially generated. The arrows shown in Figures 17–19 under the precursor heterocluster ion energy level indicate the direction the precursor level would have to be destabilized, relative to the fixed product levels, in order to account for the increase in the measured relative k^{tot}.

5. Conclusions

On the basis of our experimental results and available thermochemical data, we have ascertained the systematics of ion–molecule reactions for heteroclusters consisting of CH_3Cl and CH_3I with various oxy compounds. They can be summarized as follows.

(1) The molecule with the lowest IP is the one which will be ionized initially in the heterocluster.

(2) If the ion in the heterocluster is CH_3I, only unimolecular fragmentation occurs, with the possibility of energy transfer to the oxy compound (inducing fragmentation of it as well). The fragmentation of the oxy compound A becomes less likely as the cluster size increases.

(3) If the initial ion generated is either that of CH_3Cl or A, then the principal process will be hydrogen transfer to the ion from some neutral molecule within the heterocluster. The ion–molecule reaction competes so effectively with fragmentation that the latter is a minor process, occurring only for small clusters ($n < 3$).

(4) The reactivity for heterocluster ions appears to be much greater than for the corresponding homocluster ions. This has been explained as resulting from the fact that the heterocluster ion is less stable than the homocluster ion, which implies that the barrier for reaction is also reduced.

(5) In the case of the homoclusters, increasing the cluster size tends to reduce the relative reaction rate. However, in the case

(59) Rosenstock, H. M.; Draxl, K.; Steiner, B. W.; Herron, J. T. *J. Phys. Chem. Ref. Data, Suppl.* **1977**, *6*, No. 1.
(60) Trott, W. M.; Blais, N. C.; Walter, E. A. *J. Chem. Phys.* **1978**, *69*, 3150.

of heteroclusters, the relative reaction rate *increases* as a function of cluster size. This may be due to a reduction in the stability of the heterocluster ion with cluster size (in contrast to the situation for homoclusters).

(6) In the case of heterocluster ions it is possible for the initial ion to abstract a hydrogen from each of two different molecules. We find that the branching ratios depend in a statistical manner on the M/A ratio, i.e., the composition of the cluster. Increasing the proportion of one molecule increases the relative rate of formation of the product resulting from that molecule.

(7) The protonated cluster ion can undergo additional (possibly termolecular) ion–molecule reactions which can eliminate either HX or CH_4. In addition, for the case of dimethyl ether (and CH_3F[29]), novel termolecular reactions also occur, producing new product ions. It is speculated that they arise because of the solvated environment of the cluster, the exothermic nature of the precursor reactions, and the very stable ion products formed.

Acknowledgment. This research has been supported by NSF Grant CHE83-16205, hereby gratefully acknowledged. The authors thank T. J. Curtiss, S. R. Gandhi, and Qixun Xu for their work in connection with the design and construction of the molecular beam machine. We also thank Prof. Tomas Baer for a useful suggestion concerning the stability of dimer ions.

Solvent Bandwidth Dependence and Band Asymmetry Features of Charge-Transfer Transitions in *N*-Pyridinium Phenolates

A. M. Kjaer and J. Ulstrup*

Contribution from the Chemistry Department A, Building 207, The Technical University of Denmark, 2800 Lyngby, Denmark. *Received August 25, 1986*

Abstract: We have investigated the shape of the solvatochromic absorption band for "Betaine-26" 2,4,6-triphenyl-*N*-(di-*tert*-butyl-4-hydroxyphenyl)pyridinium ion in a range of polar, apolar, protic, and aprotic solvents. Multiphonon band theory, including both molecular modes and a vibrationally dispersive solvent, indicates that the solvents fall in three categories: (1) The bandshape for polar, aprotic solvents is well reproduced by that for a structureless continuous dielectric and a single high-frequency molecular mode. Solvent broadening correlates with $\epsilon_o^{-1} - \epsilon_s^{-1}$, ϵ_o being the optical and ϵ_s the static dielectric constant. The molecular frequency, Ω_c, and displacement, Δ_c, are not very solvent dependent, emphasizing their molecular character, and the value $\Omega_c \approx 1600\ cm^{-1}$ suggests that C–O, C–N, and C–C stretching is involved. (2) Bands for apolar, aprotic solvents correspond to the same model. Ω_c and Δ_c are again not very solvent dependent and coincide with the values for polar aprotic solvents. The solvent broadening is solvent independent, and wider than that for a structureless dielectric. This points to multipolar, dispersive, pressure, or pseudopotential forces as coupling mechanisms. (3) The bandshape for normal alcohols can only be reproduced by a model resting on two molecular modes and a vibrational high-frequency solvent "tail". Broadening, asymmetry, molecular frequencies, and deuterium isotope effects trace the protic solvent spectral entanglement to coupling between betaine-26 and a local mode group with features of both O–H stretching and bending and of librational solvent motion.

I. Introduction

Molecular solute charge transfer transitions between donor (ground state) and acceptor (excited state) orbitals exposed to the external solvent are strongly coupled to environmental polarization fluctuations. Such systems are, for example, donor–acceptor complexes,[1-3] ion pairs,[4-14] mixed-valence compounds,[15-24] and certain large organic aromatic molecules.[25-33] Most directly, and least dependent on particular solvent models, strong coupling is reflected by time-resolved fluorescence where an excited state potential surface is strongly displaced relative to the ground state surface along a suitably constructed set of solvent nuclear modes and relaxes along these coordinates subsequent to excitation, the relaxation time being correlated to the solvent dielectric relaxation times.[29-33]

Strong solute–solvent coupling charge transfer absorption band profiles are also characterized by solvent-induced band maximum, bandwidth, and bandshape features. With few exceptions such effects have been ascribed, either to inhomogeneous broadening or to specific molecular effects such as hydrogen bonding, handled largely in a qualitative fashion. Dynamic solvent effects and solute

(1) Briegleb, G. *Electronen-Donator-Akceptor-Komplekse*; Springer-Verlag: Berlin, 1961.
(2) *Molecular Complexes*; Foster, R., Ed.; Elek Science: London, 1974; Vol. 1 and 2.
(3) Foster, R. *J. Phys. Chem.* **1984**, *84*, 2135.
(4) Kosower, E. M. *J. Am. Chem. Soc.* **1958**, *80*, 3253.
(5) Kosower, E. M.; Skorcz, J. A. *J. Am. Chem. Soc.* **1960**, *82*, 2195.
(6) Mackay, R. A.; Landolph, J. R.; Poziomek, E. J. *J. Am. Chem. Soc.* **1971**, *93*, 5026.
(7) Dance, I. G.; Solstad, P. S. *J. Am. Chem. Soc.* **1969**, *91*, 7256.
(8) Nakahara, A.; Wang, J. H. *J. Phys. Chem.* **1963**, *67*, 496.
(9) MacFarlane, A. J.; Williams, R. J. P. *J. Chem. Soc., Dalton Trans.* **1969**, 1517.
(10) (a) Toma, H. E. *Can. J. Chem.* **1979**, *57*, 2079. (b) Toma, H. E. *J. Chem. Soc., Dalton Trans.* **1980**, 471.
(11) Curtiss, J. C.; Sullivan, B.; Meyer, T. J. *Inorg. Chem.* **1980**, *19*, 3833.
(12) Curtiss, J. C.; Meyer, T. J. *Inorg. Chem.* **1982**, *21*, 1562.
(13) Kristjansson, I.; Ulstrup, J. *Chem. Scr.* **1985**, *25*, 58.
(14) Kjaer, A. M.; Kristjänsson, I.; Ulstrup, J. *J. Electroanal. Chem.* **1986**, *204*, 45.
(15) (a) Hush, N. S. *Prog. Inorg. Chem.* **1967**, *8*, 391. (b) Hush, N. S. *Electrochim. Acta* **1968**, *13*, 1005.
(16) Tom, G.; Creutz, C.; Taube, H. *J. Am. Chem. Soc.* **1974**, *96*, 7828.
(17) (a) Taube, H. *Ber. Bunsenges. Phys. Chem.* **1972**, *76*, 964. (b) Taube, H. *Adv. Chem. Ser.* **1977**, *162*, 127. (c) Taube, H. In *Tunneling in Biological Systems*; Chance, B., DeVault, D. C., Frauenfelder, H., Marcus, R. A., Schrieffer, J. R., Sutin, N., Eds.; Academic: New York, 1979; p 173.
(18) Meyer, T. J. *Acc. Chem. Res.* **1978**, *11*, 94.
(19) Powers, M. J.; Salomon, D. J.; Callahan, R. J.; Meyer, T. J. *J. Am. Chem. Soc.* **1976**, *98*, 6731.
(20) (a) Powers, M. J.; Meyer, T. J. *J. Am. Chem. Soc.* **1978**, *100*, 4393. (b) Powers, M. J.; Meyer, T. J. *J. Am. Chem. Soc.* **1980**, *102*, 1289.
(21) German, E. D.; Kuznetsov, A. M. *Electrochim. Acta* **1981**, *26*, 1595.
(22) Creutz, C. *Prog. Inorg. Chem.* **1983**, *30*, 1.
(23) (a) Ludi, A. In *Mixed-Valence Compounds*; Brown, D. B., Ed.; Reidel: Dordrecht, 1980, p 25. (b) Joss, J.; Bürgi, H. B.; Ludi, A. *Inorg. Chem.* **1985**, *24*, 949 and references there.
(24) Kornyshev, A. A.; Ulstrup, J. *Chem. Phys. Lett.* **1986**, *126*, 74.
(25) Dimroth, K.; Arnoldy, G.; von Eichen, S.; Schiffer, G. *Ann. Chem.* **1957**, *604*, 221.
(26) Dimroth, K.; Reichardt, C.; Siepmann, T.; Bohlmann, F. *Ann. Chem.* **1963**, *661*, 1.
(27) Dimroth, K.; Reichardt, C.; Schwieg, A. *Ann. Chem.* **1963**, *669*, 95.
(28) Reichardt, C. *Angew. Chem.* **1965**, *77*, 30.
(29) Grabowski, Z.; Rothiewicz, K.; Siemiarczuk, A.; Cowley, D. J.; Baumann, W. *Nouv. J. Chim.* **1979**, *3*, 443.
(30) Pettig, W. *J. Lumin.* **1980**, *26*, 21.
(31) Wang, Y.; Eisenthal, K. B. *J. Chem. Phys.* **1982**, *77*, 6076.
(32) (a) Kosower, E. M.; Huppert, D. *Chem. Phys. Lett.* **1983**, *96*, 443. (b) Giniger, R.; Huppert, D.; Kosower, E. M. *Chem. Phys. Lett.* **1985**, *118*, 240.
(33) Villayes, A. A.; Boeglin, A.; Lin, S. H. *J. Chem. Phys.* **1985**, *82*, 4044.

0002-7863/87/1509-1934$01.50/0